Description of Electron Delocalization via the Analysis of Molecular Fields

Gabriel Merino,*[,†,§] Alberto Vela,[‡] and Thomas Heine*[,†]

Institut für Physikalische Chemie und Elektrochemie, TU Dresden, D-01062 Dresden, Germany, and Departamento de Química, Centro de Investigación y de Estudios Avanzados, A. P. 14-740, México, D.F. 07000, México

Received December 2, 2004

Contents

* To whom correspondence should be addressed. E-mail addresses: gmerino@quijote.ugto.mx; Thomas.Heine@chemie.tu-dresden.de.
† TU Dresden.
§ Permanent address: Facultad de Química, Noria Alta s/n. Universidad de Guanajuato, Guanajuato 36050, Mexico.
‡ Centro de Investigación y de Estudios Avanzados.

1. Introduction

Chemists have been fascinated for a long time with electron delocalization in covalently linked molecules, and especially with the prototypical phenomenon of aromaticity. Even though the introduction of this concept in chemistry is quite old, its definition and conceptualization is not free of controversy. One can start with the definition provided by IUPAC in 1994: electron delocalization is "a quantum mechanical concept most usually applied in organic chemistry to describe the pi bonding in a conjugated system. This bonding is not localized between two atoms: instead, each link has a fractional double bond character or bond order".[1] Consequently, the difference between the energy of the delocalized system and the energy of a hypothetical structure that contains formally localized single and double bonds is normally used as a model to measure electron delocalization. These energetic effects are more tangible in aromatic systems and in symmetrical molecular entities where a lone pair of electrons or a vacant π-orbital is conjugated with a double bond.

The concept of electron delocalization is readily used in all areas of chemistry and in condensed matter physics, where it is the cornerstone for models to treat metals. It should be pointed out that electron delocalization is not directly accessible in experiment, but its consequences are. This experimental impossibility of measuring electron delocalization directly has opened the door to many controversial issues and discussions around this key concept in electronic structure theory. Thus, it is not surprising to find many attempts to define this term depending on the grounds of different approaches to describe the electronic structure problem. Coulson illustrated clearly this point for benzene: "There is an interesting contrast between the valence bond and molecular orbitals descriptions of benzene. Both require complete delocalization, but whereas the VB method introduces it by superposition of Kekulé (and other) structures, in the MO method there is nothing that even remotely resembles a structure. This situation warns us one more against any too literal belief in the reality of our structure".[2] Thus, assigning an unequivocal and absolute meaning to electron delocalization and especially to the closely related term "aromaticity" is risky. Lloyd and Marshall elegantly condense this position: "The term aromatic was interpreted at different times in terms of molecular structure, of reactivity and of electronic structure, and, in consequence, there has been much confusion

10.1021/cr030086p CCC: $53.50
Published on Web 09/27/2005

Gabriel Merino was born in Puebla, Mexico, in 1975. He was educated at Universidad de las Américas-Puebla and Cinvestav (where he studied with Prof. Alberto Vela). After a 2-year postdoctoral stay at TU-Dresden, Germany, where he worked with Prof. Gotthard Seifert and Dr. Thomas Heine in several aspects of magnetic response, he joined the Department of Chemistry at Universidad de Guanajuato. His research interests include design of molecules containing planar tetracoordinate carbon atoms, study of molecular scalar fields, and electron delocalization.

Alberto Vela was born in Mexico City. He received his B.E. in the Faculty of Chemistry-UNAM and his Ph.D. in 1988 in the department of Chemistry at UAM-Iztapalapa, under the supervision of Prof. J. L. Gazquez, learning the fundamentals of density functional theory. In 1993, he was a visiting researcher, for almost 2 years, in Prof. Dennis R. Salahub's group where he started his journey with the program deMon. From 1983 until 1997, he was full professor of the department of Chemistry at UAM-I where he participated in the creation of the Theoretical Physical Chemistry group. After 14 years in UAM, he moved to the Department of Chemistry at Cinvestav where he started the Theoretical Chemistry group in 1997, where he is full professor of the Department of Chemistry. His research interests are the development and applications of density functional theory.

over its precise meaning and definition. We suggest that because of this confusion, it would be better if the use of the term "aromatic" was discontinued, safe perhaps with its general and original connotation of "perfumed", and that it should pass with other technical terms which have outlived their precision and usefulness to the realm of the historian of chemistry".[3]

In view of these problems of subjectivity, it is remarkable that the concept of electron delocalization (and aromaticity) is useful to rationalize and understand the structure and reactivity of many molecular entities. As a result, the concept of electron delocalization is truly a cornerstone, and all treatments of the subject from the simple to the advanced rely heavily on some sort of classification of compounds

Thomas Heine was born in Seehausen (Germany) in 1970. He studied physics at TH Merseburg and TU Clausthal (Germany), and received his master degree at the Institute of Theoretical Physics in 1995, under the supervision of Prof. Lothar Fritsche. During his time as a Ph.D. student (1995–1999) at TU Dresden (Germany), Institute of Theoretical Physics, supervised by Prof. Gotthard Seifert, he worked as visiting researcher at the Department of Chemistry, University of Montreal (Canada), in the group of Prof. Dennis Salahub and at the School of Chemistry, Exeter University (U.K.), in the group of Prof. Patrick Fowler. After postdoctoral stages at the Department of Chemistry, University of Bologna (Italy), working with Prof. Francesco Zerbetto, and the Department of Physical Chemistry, University of Geneva (Switzerland), in the group of Prof. Jacques Weber, he joined the Institute of Physical Chemistry and Electrochemistry of TU Dresden in 2002. His research interests are the development of methods of theoretical chemistry, including density-functional theory and tight-binding methods, and their application, in particular to study magnetic properties of molecules and solids.

according to a given degree of delocalization. Therefore, the concept per se is strong enough motivation that justifies the continuous effort of many researches to develop it in a more general way.

Clearly, one line of investigating electron delocalization is through the MO analysis. A characteristic element of molecular orbitals is that, by construction, they are delocalized over the whole molecule, adopting the symmetry of the molecular framework. This feature is in contrast with many widely used chemical concepts, such as chemical bond, lone pair, and chemical group, which all have a local character. Since the molecular electronic distribution is invariant with respect to any unitary transformation of the original canonical orbitals used, many attempts to build a model of the chemical bond and electron delocalization have relied on different schemes of localization. At the correlated levels of the electronic distribution definition, a simple and clear decomposition into local orbitals is no more valid, however. A more general definition of MOs, the natural orbitals, has been developed.[4] This approach permits a recovery of the local descriptions previously introduced at the Hartree−Fock (HF) level only and gives additional robustness to the chemical concepts by describing molecular bonding within the local orbitals formalism. However, it is not a unique possibility.

An alternative to the wave function description of a quantum system is density matrix theory. As it is well-known and thoroughly described in several texts,[5−7] for a nonrelativistic Hamiltonian with two-body interactions, the energy of the system can be exactly expressed by the one-electron density matrix. The diagonal elements of the first-order reduced

density matrices correspond to the electron density, while those corresponding to the second-order reduced density matrices describe the electron pair density.

The electron density is a scalar field that can be experimentally accessed[8] and whose prominent role in the description of many-body problems, such as chemical bonding, is supported by the Hohenberg and Kohn theorems.[9] Convinced about the relevance of the electron density in the description of chemical phenomena, in the 1970s, Richard Bader presented a theory of the chemical bond solely supported on this scalar field, putting forward the idea of analyzing the topology of the charge distribution in real space. Anticipating our conclusion, the electron delocalization is a notoriously difficult concept to extract directly from the topology of the electron density. However, it is important to note that the mathematical apparatus provided by the topological analysis is not restricted to the electron density. It can be applied to other molecular fields such as the molecular electrostatic potential, $V(\mathbf{r})$,[10] the electron localization function, ELF($\mathbf{r}$),[11] the Laplacian of the electron density, $\nabla^2\rho(\mathbf{r})$,[12] the electronic current density,[13] or the Laplacian of the conditional pair density.[14]

There are some reviews on the analysis of molecular scalar fields; however, they do not examine in detail electron delocalization.[8,15−19] The present review focuses on the description of electron delocalization via the analysis of molecular fields. We begin with several important remarks about the analysis of molecular fields to define the compass and character of our discussion. We try to cover a large spectrum of functions, starting with the electron density and the Fermi hole, following with the Laplacian of the electron density, and ending with the electrostatic potential. It is important to mention that some molecular fields, particularly the electron localization function,[20] are not discussed in the present review because they are the main subject of other contributions in this issue of *Chemical Reviews*. Finally, the concept of electron delocalization is inevitable linked to the localization of electron pairs (Lewis model), whereby in each section both phenomena will be discussed.

2. Basic Concepts

In this section, a precise definition of what is to be understood for a topological analysis of a scalar field in chemistry is presented. For the sake of completeness, a scalar field, $f(\mathbf{r})$, is the mapping $\mathscr{R}^3 \rightarrow \mathscr{R}$ that assigns a real number to each point in space. From the strict mathematical point of view, topological analysis is the branch of mathematics that deals with the investigation of the analytical properties (curvature, connectivity, punctures, homotopies) of bodies to distinguish different kinds of manifolds. In this sense, it is unfortunate that in chemistry the term topological analysis does not reflect completely the mathematical definition. Before proceeding to the definitions of the topological analysis of a molecular scalar field, it is necessary to introduce several basic concepts.

The topological properties of a scalar field are determined by the analysis of its associated gradient vector field.[21] The first important feature is the location in space of the critical points (CPs). A critical point is a point $\mathbf{r}_c \in \mathscr{R}^3$ where the gradient of the scalar field $f(\mathbf{r})$ vanishes:

$$\nabla f|_{\mathbf{r}_c} = 0 \tag{1}$$

Thus, a CP is a point where the corresponding scalar field has an extremum. To characterize the critical points, one assumes that, for a sufficiently well-behaved scalar field, the Hessian of the field,

$$\mathbf{H}_{xyz} = \begin{pmatrix} \partial^2_{xx} f & \partial^2_{xy} f & \partial^2_{xz} f \\ \partial^2_{yx} f & \partial^2_{yy} f & \partial^2_{yz} f \\ \partial^2_{zx} f & \partial^2_{zy} f & \partial^2_{zz} f \end{pmatrix} \tag{2}$$

where $\partial^2_{\alpha\beta}$ is a shorthand notation for the second partial derivative with respect to the Cartesian coordinates α and β, is a real and symmetric matrix. Consequently, at any given point $\mathbf{r} \in \mathscr{R}^3$, diagonalization of the Hessian matrix $\mathbf{H}_{xyz}$ is possible and yields three real eigenvalues, λ_i. The corresponding eigenvectors are the principal axes. The characterization of a CP depends on its rank and signature. The rank, R, of a CP is the number of eigenvalues that are different from zero, and the signature, S, is the algebraic sum of the signs of the eigenvalues:

$$S = \sum_{i=1}^{3} \mathrm{sign}(\lambda_i) \tag{3}$$

Thus, a CP is classified by the ordered pair (R, S). For a three-dimensional function, the rank can take the values 0, 1, 2, and 3. A (3, −3) is a local maximum, a (3, −1) is a maximum in two directions and a minimum in the other direction, a (3, +1) is a minimum in two directions and a maximum in the other direction, and finally, a (3, +3) is a local minimum. The (3, −1) CP is particularly important in the topological analysis of the electron density since this point is associated with the formation of a bond and because of this, it has been named a bond critical point (BCP).

A gradient path is defined by creating a trajectory following the gradient of the field in each point. Because gradient vectors have a direction, gradient paths also have one: they can go uphill or downhill. All gradient paths are directed to an attractor. Therefore, gradient paths have an end and a starting point. Bader proposed that the presence of a gradient path of the electron density connecting two atoms provides a universal indicator of bonding between the atoms that are linked by this path,[22] a statement that has been the subject of some controversy (see refs 23 and 24). A molecular graph is defined as the network of gradient paths that link neighboring nuclei (Figure 1).

Finally, the molecular space is partitioned into "basins" Ω_X, each one corresponding to the space

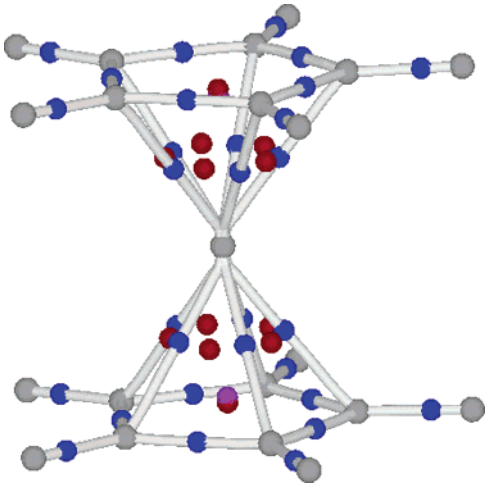

Figure 1. Molecular graph of ferrocene. Blue, red, purple, and gray spheres indicate the positions of (3, −1), (3, +1), (3, +3), and (3, −3) CPs, respectively.

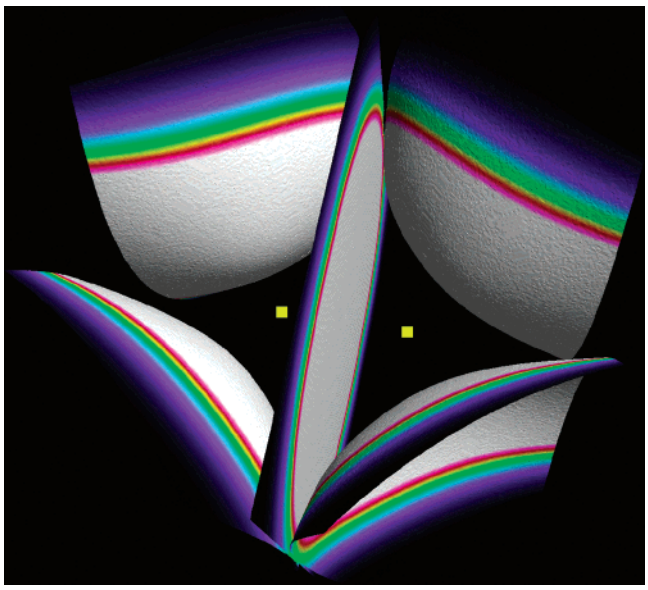

Figure 2. Zero flux surface of ethylene. Yellow squares indicate the position of the carbon atoms. Reprinted with the kind permission of Prof. Chris Henze.

spanned by the set of paths ending at an attractor. The surfaces separating basins are mathematically defined by trajectories of ∇f that terminate at a (3, −1) critical point (Figure 2). Since trajectories never cross, an interatomic surface is endowed with the property of zero-flux, that is, a surface that is not crossed by any trajectory of ∇f:

$$\nabla f(\mathbf{r})\cdot\mathbf{n}(\mathbf{r}) = 0 \tag{4}$$

where $\mathbf{n}(\mathbf{r})$ is a unit vector perpendicular to the surface at point $\mathbf{r}$. Equation 4 is the boundary condition for the definition of a quantum open system—one whose expectation value obeys the same theorems as do those of the total system of which they are a part.[17] Thus, the gradient paths of the scalar field induce, in a natural way, a partitioning of space that for fields with attractors at the atomic nuclei positions is in atomic resolution. Then, any property P that is calculated by the normal expectation value of the associated Hermitian operator,

$$P = \langle\Psi|\hat{P}|\Psi\rangle \tag{5}$$

can be written as a sum over the basins $\{\Omega_A\}$ generated by the space partitioning,

$$P = \sum_A \langle\Psi|\hat{P}|\Psi\rangle_{\Omega_A} \tag{6}$$

where each integration is done over the Ω_A basin. If $\hat{P}$ is a local and one-body operator, then eq 6 can be expressed in terms of the electron density:

$$P = \sum_A P_A = \sum_A \int_{\Omega_A} \mathrm{d}\mathbf{r}\, P(\mathbf{r})\, \rho(\mathbf{r}) \tag{7}$$

3. Electron Density

Typically, a theoretical investigation that attempts to elucidate the nature of the existent interactions in a molecular system uses one or several of the Hilbert space analyses of the wave function (basis set expansions) or the first-order density matrix. The shortcomings of these approaches are well-known and in several cases the arbitrary partition of the density matrix generates contradictory results regarding the nature of chemical bonds.[4,25] According to the first Hohenberg−Kohn theorem,[9] the ground-state properties of a many-electron system are uniquely determined by the electron density, $\rho(\mathbf{r})$. In the 1970s, partially inspired by the seminal works of Hohenberg, Kohn, and Sham,[9,26] Bader and co-workers provided chemists a valuable tool for the examination and description of the nature of the chemical bond in terms of the topological analysis of the electron density as described in the previous section. In recent years, this approach has become a standard method to explore the nature of the chemical bond in molecules and extended systems. The reader interested in further details is directed to refs 15−17 and 27−29.

Chemists have long sought a way to relate the properties of critical points of the electron density to electron delocalization. In the 1980s, σ-aromaticity of cyclopropane was rationalized in terms of the ellipticity of the density at its critical points.[30] Recently, several experimental and theoretical studies have considered critical point descriptors of the electron density evaluated at the (3, −1) CPs (namely, the electron density, the Laplacian of the electron density, and ellipticity) as parameters reflecting the electron delocalization. Unfortunately, to date, there is no solid relationship between these descriptors and electron delocalization. It should be noted that almost all studies concerned with electron delocalization that use some kind of analysis of the electron density have also to rely on another study of their orbitals or magnetic or energetic properties to support their conclusions. The reason is that the electron density shows, in general, local maxima only at the nuclear positions[17] but by itself does not provide any signal of the spatially localized bonded and nonbonded electron pairs. Recall that the spatially localized patterns of the orbital densities as well as their related node structures vanish when they are summed

to build the electron density. Nevertheless, the critical point descriptors of electron density (CPDEDs) mentioned above, as well as others, are currently used, and in several cases, they seem to be capable of describing the degree of the electron delocalization in a molecule.

3.1. Critical Point Descriptors

What is a critical point descriptor? We are interested in critical points of the electron density, that is, in points where the gradient of the density is zero, $\nabla\rho(\mathbf{r}) = 0$. Once the critical points have been localized, various properties can be evaluated at their position in space. Among these, ρ_{CP}, the charge density at the CP, is of paramount importance. There has been an attempt to relate the electron density at the (3, −1) CPs, ρ_b, to the bond order, n.[31] Two quantities derived from the eigenvalues of the Hessian are also used to characterize the critical points. They are the ellipticity, ϵ, and the Laplacian of the charge density, $\nabla^2\rho$, which is the trace of the Hessian. The latter parameter provides a measure of how much ρ is concentrated or depleted in a given point.[12] All these critical point descriptors will be discussed in more detail in the next sections.

To illustrate the usage of the CPDEDs in describing the delocalization problem, let us consider benzene, whose aromaticity can be viewed as a complete delocalization of the π electrons over the carbon skeleton. In terms of the CPDEDs, the limiting case of complete delocalization of the π electrons in a cyclic system corresponds to each bond having the same values for n, $\nabla^2\rho$, and ϵ.[31] Benzene perfectly meets these conditions. However, it should be pointed out that there could be systems lacking complete delocalization but fulfilling the criteria described with the CPDEDs.

In 1997, Howard and Krygowski performed HF/6-31G** calculations on some polycyclic aromatic hydrocarbons (PAHs).[32] They found that the CPDEDs at the (3, −1) CPs are linearly related to the bond lengths. The CPDEDs were also evaluated at the (3, +1) CPs. The values correlate closely with two different aromaticity indices: the harmonic oscillator model of aromaticity (HOMA) parameter[33] and the nucleus-independent chemical shifts (NICS).[34] However, the curvature of the electron density perpendicular to the ring plane, λ_3, provides the best correlation with the HOMA and NICS indices. Based on these results, Howard and Krygowski proposed a ring critical point index as a way to quantify the degree of electron delocalization in aromatic molecules.

Both examples show how the CPDEDs have been used to describe electron delocalization. A large number of studies that attempted to relate these descriptors to electron delocalization were published in the last 2 decades, most of them focusing their attention on the electron density and the ellipticity. However, as it will be seen below, other concepts that are related to the electron density such as the surface delocalization, the ellipticity profile, and the bond order have been introduced more recently to gain in the understanding of electron delocalization.

3.2. Applications of the Critical Point Descriptors of Electron Density

3.2.1. Aromatic Molecules

Mo et al. studied structures and properties of mono-, bis-, and tris-annulated benzocyclopropenes (see Scheme 1) and their fluorinated derivatives.[35]

Scheme 1

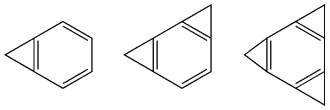

They showed that the Mills−Nixon type of bond length alternation is apparent in fused hydrocarbons despite the existing bent bonds. A reverse Mills−Nixon effect was detected in the fluorine-substituted compounds. It appears that fluorination "freezes" that particular structure, which involves localized double bonds at coalesced (fused) positions. This conclusion was interpreted in terms of rehybridization at the carbon junction atoms and π bond orders and further supported by the values of the CPDEDs. Clearly, the fusion of small rings affects the properties of the aromatic benzene nucleus in a significant way.[35] The group of Eckert-Maksic made a similar analysis in silacyclopropabenzenes[36] and cyclopropanaphthalenes.[37]

Roversi et al. have determined the experimental electron density of citrinin (Scheme 2).[38] The almost

Scheme 2

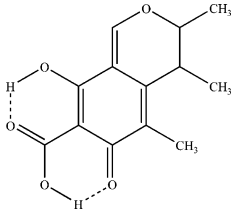

planar arrangement seems to be supported by π-delocalization extended along both sides of the ring's skeleton. This experimental study shows how the electron density at the (3, −1) CPs increases on passing from the single to double bonds. Clearly, the ellipticities reflect an increased charge contraction toward the corresponding (3, −1) CPs and also enhanced π-bond character.

An experimental analysis of the electron density of the squarate and croconate dianions (Scheme 3)

Scheme 3

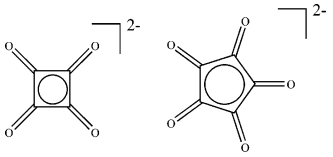

was carried out by Ranganathan and Kulkarni.[39] They analyzed the CPDEDs at the (3, +1) CP and argued that one can distinguish aromatic and nonaromatic systems by plotting the $\nabla^2\rho_b$ vs ρ_b: The aromatic rings fall in a region where the Laplacian

is roughly proportional to the density, and the nonaromatics show no definitive trend.

3.2.2. Heterocycles

Molina et al. analyzed the aromaticity of three-membered heterocycle (N, P, and As) oxides using the CPDEDs and ELF(**r**).[40] They found a high electron delocalization only for the unsaturated phosphorus and arsenic oxide derivatives. Negative hyperconjugative effects in the N−O bond formation explain the nonaromaticity of the amine oxide derivatives. Raos et al. have studied the conformational states of bithiophene derivatives, as a function of the type and degree of substitution.[41] In particular, the topological analysis of the electron density supports that the interring conjugation is not the main driving force for planarization, although it is certainly important as far as the transition barrier height is concerned.

On the basis of the experimental CPDEDs, several heterocycles have been studied. For example, the experimental ρ_b values at the C−N bonds of imidazole and triazole[42,43] are statistically equal. Consequently, these bonds cannot be considered as double or single, which immediately suggests an evident degree of electron delocalization. However, the Laplacian and ellipticities do not confirm the picture based on ρ_b. Since in the crystal the two terminal N atoms are donors and acceptors in strong hydrogen bonds, the crystalline environment is probably balancing the bonds and enhancing the aromatic character of the rings.[42,43] Bianchi et al. studied the topological properties of 4-cyanoimidazolium-5-olate (Scheme 4).[44]

Scheme 4

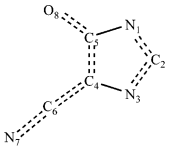

They concluded that this molecule could be described as a two-conjugated system (N1−C2−N3 and O8−C5−C4−C6−N7) linked by single C−N bonds. This feature could also be attributed to the effect of the crystal environment, since each of the N atoms of the N−C−N skeleton is involved as a donor in strong hydrogen bonds.[44]

A typical model of biological processes involving proton transfer via tautomerism (Scheme 5) is 2-pyridone. Yang and Craven studied this molecule in the solid phase at 123 K. Under these conditions, the *lactam* form is favored.[45] The values of ρ_b at the C−C bonds are higher than expected for a single bond and lower than for the double bond. In addition, a statistically uniform distribution of the ellipticities among C−C and C−N bonds was found. Thus, all

Scheme 5

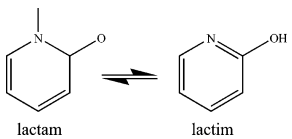

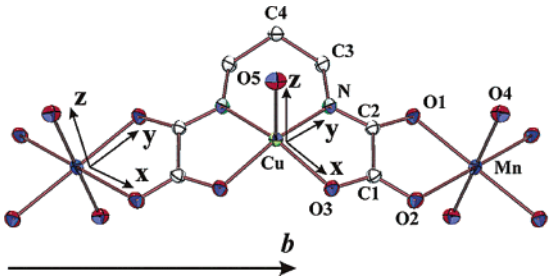

Figure 3. ORTEP view and labeling of the chain structure. Thermal displacement ellipsoids are plotted at the 50% probability level. Hydrogen atoms and noncoordinated water molecules are omitted for clarity. Mn and Cu local coordinate systems are also given. Reprinted with permission from ref 51. Copyright 2004 American Chemical Society.

indications point to π-delocalization over the entire ring, that is, a tendency toward the *lactim* tautomer, in agreement with the intermolecular hydrogen-bonding pattern.

Further analysis of the CPDEDs has been made by Gatti et al. for bipyrroles,[46] by Nyulaszi for pentaphospholate,[47] and by Pizzonero et al. for enaminonitriles.[48]

3.2.3. Transition Metal Complexes

Recently, the group of Lecomte has used the analysis of the experimental electron density to obtain insight into the interaction mechanisms of molecular magnetic compounds (organic free radicals, coordination compounds, and organometallic complexes).[49−53] A beautiful example is the MnCu(PBA)-$(H_2O)_3 \cdot 2H_2O$ compound (Figure 3),[51] where PBA stands for 1,3-propylenebis(oxamato). In this bimetallic chain compound, the CPDEDs of (3, −1) CPs of the oxamato bridge show characteristic features of conjugation effects: short bond lengths, high electron densities, high Laplacians, and high ellipticities. This electron conjugation is necessary to propagate the interactions along the chain, and it can be related to a superexchange Mn−Cu coupling mechanism, in addition to the electron (spin) delocalization. Clearly, the intrinsic complexity of these transition metal systems has been a hurdle to calculation and analysis of their critical point descriptors. The developments in theories, algorithms, and computational infrastructure allow us to believe that in the very near future more work along these lines will be possible.

3.2.4. Carbocations

Carbonium ions are important species involved in acid-catalyzed transformations. They are formed by the protonation of alkanes in liquid superacids, and there is evidence for the formation of pentacoordinate carbonium ions.[54] These species contain three-center two-electron bonds (3c−2e) and can be generated upon the insertion of a proton or a carbenium ion into the C−H or C−C bonds. The group of Jubert has analyzed the electron distribution of $C_3H_9^+$,[55] n-$C_4H_{11}^+$,[56,57] and i-$C_4H_{11}^+$.[58] They concluded that the stability of these protonated species depends fundamentally on the way in which the charge of the cation is delocalized around the 3c−2e bonds.

The important role of back-bonding interaction in phenonium ions has been studied by del Rio et al.[59] For the phenonium ion $[C_6H_5-C_2H_4]^+$, the analysis of the Kohn−Sham orbitals and the CPDEDs shows that back-bonding from the phenyl cation moiety to the ethylene fragment determines the formation of the three-membered cycle. This makes the shielding of the *ipso* carbon atom similar to that for a sp^3 C, while an extension of the conjugation occurs as both π systems merge.

3.2.5. Hydrogen Bonds

Hydrogen bonds play a crucial role in biological systems such as proteins and DNA base pairs, and they are essential for life processes. A variety of factors may influence the features of hydrogen bonds. The delocalization of π-electrons within H-bonded systems can be among them. Gilli et al. suggested that the additional hydrogen bonding energy in the strong resonance-assisted hydrogen bond (RAHB) systems can be thought of as originating from partial charges of opposite signs present in the resonance isomer (Scheme 6).[60]

Scheme 6

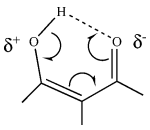

Gatti et al. noted that π conjugation on urea propagates through hydrogen bonds.[61] The group of Grabowski has studied the electron distribution in intermolecular H-bonds.[62−66] These studies support Gilli's suggestion that π-electron delocalization influences significantly the geometrical parameters and the strength of the H-bonds. In particular, the properties of the (3, −1) CPs, which result from intramolecular H-bond formations, correlate well with other measures of H-bond strength.[67,68] Furthermore, the part of the energy that is roughly responsible for the π-electron delocalization in several malonaldehyde derivatives correlates with ρ_b at the H···O bond.[69] In the same vein, Alkorta and Elguero have studied the influence of dimerization by hydrogen bonding formation of 2-hydroxypyridine and 2-aminopyridine and their corresponding derivatives.[70]

In the study of benzoylacetone (Scheme 7), the diffraction data provide support for the location of the enol hydrogen in a very flat asymmetric single minimum potential.[71,72] The electron density distribution derived from combined analysis of the neutron and X-ray diffraction data shows a large π-delocalization in the keto−enol group. Madsen et al. have found high formal charges on both the oxygens and the enol hydrogen,[71,72] reflecting the fact that the hydrogen is closely bound to two electronegative atoms. It has been concluded that the bonding of the hydrogen for this short intramolecular hydrogen bond at each side of the hydrogen has partly covalent and partly electrostatic contributions.

Scheme 7

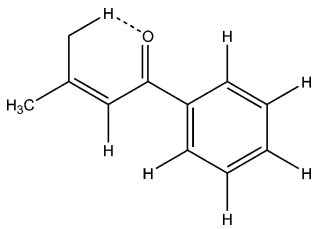

Platts and Howard studied the structure of the 1,8-bis(dimethlyamino)naphthalene (see Scheme 8) and its protonated form.[73] They found that protonation causes the molecule to become more planar, presumably due to increased localization of charge in the lone pairs of the nitrogens. The CPDEDs for C−C bonds are also closer to the corresponding values in naphthalene upon protonation, although the ellipticities do not follow this trend. Whether this corresponds to increased "aromaticity" is arguable, given that there is no agreed definition of this concept. In 1999, Mallinson et al. reported a neutron experiment together with the X-ray charge density results of 1,8-bis(dimethlyamino)naphthalene (Scheme 8).[74] Com-

Scheme 8

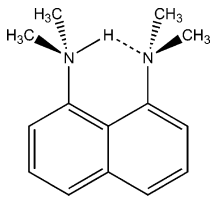

parison of the geometrical parameters obtained by a neutron experiment of the neutral and ionic species shows that upon protonation the aromatic C−C bonds become shorter while the C−N bond at the acceptor N atom lengthens. These structural changes manifest themselves in the ρ_b values, indicating that in the ionic form the conjugation, which also includes NH_2 groups, is limited to the naphthalene ring.

3.3. Surface Delocalization

Let us first define the ellipticity. In a bond with cylindrical symmetry, the negative eigenvalues of the Hessian of the electron density at the (3, −1) CP are identical, $\lambda_1 = \lambda_2$. However, if charge is preferentially accumulated in a given plane, the falloff rate of ρ from its maximum value is largest along the axis perpendicular to the plane. Hence, the magnitude of the corresponding curvature of ρ is smaller for the axis lying in the plane. If λ_2 is taken to be the value of the smallest curvature, then the ellipticity of the bond is given by the following expression:

$$\epsilon = \frac{\lambda_1}{\lambda_2} - 1 \qquad (8)$$

Essentially, the magnitude of this quantity provides a measure of the extent to which electron density accumulates in a given plane. Bader suggested that the ellipticity provides a quantitative measure of the π-character of the C−C bond and the plane of the π distribution is uniquely specified by the direction of the axis associated with the curvature of the smallest

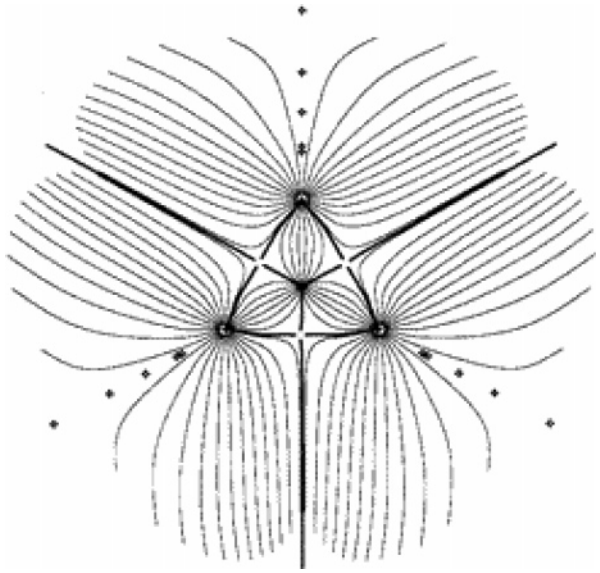

Figure 4. Gradient vector field of the electron density in cyclopropane.

magnitude, λ_2.[31] This descriptor has also been capable of describing weak intra- and intermolecular interactions[75−77] and multicenter bonding.[78−80]

The concept of σ-aromaticity has been justified in terms of ellipticity values. In 1980, Dewar and McKee suggested that cyclopropane and benzene are isoconjugate because both molecules have a sextet of strongly delocalized electrons. In this way, benzene presents a π-aromatic system, and cyclopropane can be considered to be σ-aromatic.[81] In 1983, Bader et al. observed that C−C gradient paths of cyclopropane have significant ellipticities, and that their major axes are in a plane coinciding with the ring surface (See Figure 4). This is a consequence of the proximity of the (3, +1) and (3, −1) CPs.[31] Usually, ellipticities of bonds in three-membered rings exceed those found in the double bond in ethylene.[82] However, the electron delocalization in cyclopropane is, in form and properties, different from that associated with a conjugated π system.

Cremer et al. have used the topological theory of molecular structure to provide an alternative as to whether homoconjugation is present in a given molecule.[83] Similar studies have been made by the same author for cyclo[6.2.0]decapentacene[84] and by Barzaghi and Gatti for homotropylium cation.[85] These arguments were also used to discuss the relative stability between [10]-annulene and dienocarediene as a function of ring surface.[86]

The chemistry of cyclopropane is a consequence of the high concentration of charge in the interior of the ring. Cremer et al. emphasized that the delocalization of charge in cyclopropane is necessarily two-dimensional, being a maximum in the ring surface defined by λ_1 and λ_2. The result is a surface of delocalized charge containing the ring and the C−C (3, −1) CPs.[83] In 1985, Cremer et al. extended the previous study and drew a connection between the electron distribution and σ-aromaticity of cyclopropane.[30,87] They found that the ratio of ρ_b/ρ_r (where ρ_r is the electron density at the (3, +1) CP) in cyclopropane is still 82%, while in cyclobutane or benzene it is just 33% and 7%, respectively. Thus, they concluded that "since the density distribution of benzene is a result of ribbon delocalization of π-electrons, we describe the density pattern of cyclopropane by the term surface delocalization and consider surface delocalization to arise from the (aromatic) delocalization of 6 σ-electrons in the plane of the ring".[30]

The previous model was also employed to rationalize the substituent effects on ring strain in cyclopropane.[88] In general, electropositive substituents stabilize cyclopropane due to a predominant enhancement of σ-aromaticity. The reverse is true for electronegative substituents such as F or OH. In contrast, a systematic substitution of the $-CH_2-$ fragment of cyclopropane by −NH− or −O− groups decreases the degree of electron delocalization, while the conventional ring strain energy remains almost constant.[89]

Koritsanszky et al. presented a topological study on the bullvalene molecule (Scheme 9) based on both

Scheme 9

the experimental and the theoretical electron distribution.[90] There are significant differences in the CPDEDs of the two formal single bonds; the bond next to the cyclopropane ring appears to be stronger, and it exhibits more π character than that formed by the C(sp^2) and C(sp^3) atoms. This is in accordance with theoretical and experimental observations on the conjugation effect, which is due to the unsaturated character of the cyclopropane ring.

The surface delocalization model has been applied to study the stability of boranes, carboranes,[91,92] and metallocenes.[93,94] This analysis reveals that the charge delocalization over the ring surfaces and charge accumulations in the bonds contribute to the stability of structures. Thus, the ring formations play an important role in the stabilization of these systems. Further applications of surface delocalization have been made to three-membered inorganic[95−97] and organic compounds.[35,37,98] Finally, the experimental electron density distribution maps of spiropentane, [3]rotane, [4]triangulane, and trispiro[2.0.2.1]heptane (Scheme 10) show some asymmetry with the maxima

Scheme 10

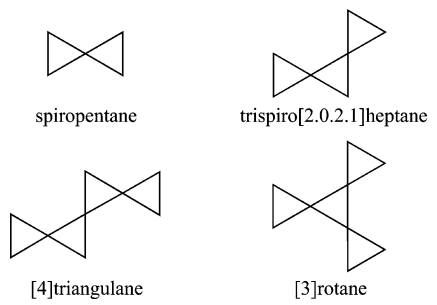

being more pronouncedly shifted outside the ring along the proximal and distal bonds.[99−101] Recent experimental results support surface delocalization of σ-electrons in cyclopropane derivatives. However,

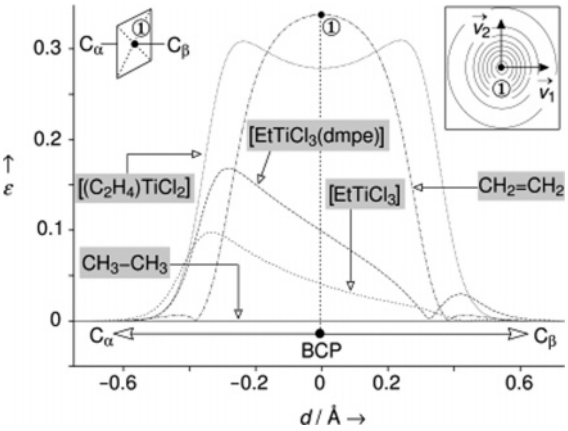

Figure 5. Ellipticity profiles along the $C_\alpha-C_\beta$ bond path of $EtTiCl_3$ and $EtTiCl_3$(dmpe) [dmpe = $Me_2PCH_2CH_2PMe_2$] in comparison with C_2H_6, C_2H_4, and $(C_2H_4)TiCl_2$. d is distance from the (3, −1) CP. Reprinted with permission from ref 109. Copyright 2003 Wiley-VCH.

it is worth noting that the surface delocalization has been almost abandoned and substituted by new orbital or magnetic explanations of the σ-aromaticity concept.[102−105]

3.4. Ellipticity Profile

Tafipolsky et al. carried out a combined experimental and theoretical charge-density study of acyclic and *N*-heterocyclic carbenes.[106] They showed that the usual analysis of CP descriptors could be misleading in estimating the degree of electron delocalization. Standard criteria of delocalization based on interpretation of the wave function may also prove misleading, being quite insensitive to changes in the electronic nature of the system. In such cases, a full bond path analysis could be more instructive and meaningful. Furthermore, CP descriptors evaluated along a full bond path present a characteristic pattern that is less sensitive to variations in the theoretical level of calculations or the choice of the experimental multipole model than are topological parameters evaluated at the (3, −1) CP alone.

Ellipticity profiles have been used to reveal the nature and extent of electron delocalization in agostic interactions (Figure 5).[107−109] They show that the agostic interaction leads to a global bonding redistribution of $\rho(\mathbf{r})$ within the metal-alkyl moiety. This redistribution is a natural feature of delocalization of the M−C bond electrons, a fact that becomes evident when the ellipticity is traced along the full $C_\alpha-C_\beta$ bond. In this sense, the asymmetry in ϵ charts the degree of π character (or deviation from σ symmetry) along a bond path, whereas the position and magnitude of the maximum value of the ellipticity, ϵ_{max}, reveals the extent of delocalization.

3.5. Molecular Similarity

Even though it is not strictly related to the description of electron delocalization by means of the CPDEDs, it is worth mentioning that recently, Popelier and O'Brien introduced an abstract space of the CPDED, called bond critical point space, to measure the similarity between molecules.[110−113] The experimental activity sequence will only be reproduced if the distance measure is confined to contributions from the BCPs from the common active center of the molecules.[110] This approach consists of three stages: the generation of geometry-optimized bond lengths and wave functions, computation of CPDEDs, and a chemometric analysis. Using similar ideas, Platts predicted hydrogen bond basicity[114] and hydrogen bond donor capacity.[115] Matta employed this quantum topological molecular similarity (QTMS) tool to predicted experimental physicochemical properties of molecules of biologic interest: amino acids, polycyclic aromatic hydrocarbons, and opiates.[116,117] Popelier and co-workers studied the toxicity of polychlorinated dibenzo-*p*-dioxins,[118] antibacterial activity of nitrofuran derivatives, antitumor activity of (*E*)-1-phenylbut-3-en-ones,[113] and Hammett constants of mono-[110] and polysubstituted benzoic acids, phenylacetic acids, and bicyclocarboxylic acids.[118]

3.6. Nucleus-Independent Chemical Shifts and (3, +1) Critical Points

An interesting combination of the topological analysis of the charge density and nucleus-independent chemical shifts (NICS) computations was proposed in the late 1990s: The position at which a NICS computation is carried out is chosen often in an arbitrary way, for example, by averaging the positions of the heavy atoms of the ring.[34] For highly symmetric molecules, this option corresponds to the (3, +1) CP of the electron density and even of the shielding density.[119] However, for more complex molecules or multiple ring systems, the selection of a meaningful position for the NICS computation is not obvious anymore, and to gain a better understanding, NICS values are sometimes computed on a grid.[120,121] It appears eligible to establish a well-defined point for the computation of a NICS value characterizing a ring. One of the possibilities to define such a site in an unambiguous way is to use the (3, +1) CPs of the electron density. In fact, this strategy has been followed in the past decade quite frequently.[122−135] However, since NICS is a magnetic criterion, the choice of the NICS site might be improved by choosing a critical point of a field that is related to the applied magnetic field, such as the current density,[136] the magnetic shielding function,[137] or the induced magnetic field.[119] Since these combinations are computationally demanding or are very recent developments, these studies are still to be done.

3.7. Bond Order

The earliest and most widely known attempt to quantify the bond order of a chemical bond is Pauling's two-parameter proposal:[138]

$$n = \exp[(r_0 - r)/a] \tag{9}$$

where $a \approx 0.3$ for any type of bond, and r_0 is an idealized single bond length for the treated bond type under scrutiny. By analogy with Pauling's relationship, Bader defined a carbon−carbon bond order, n_B,

in terms of the values of density at the (3, −1) CP as

$$n_B = \exp[A(\rho_b - B)] \quad (10)$$

where A and B are constants that are adjusted to yield bond orders of 1.0, 1.6, 2.0, and 3.0 for ethane, benzene, ethylene, and acetylene, respectively.[31] This definition has found considerable use to examine homoaromaticity[83] and electronic reorganization during the progress of chemical reactions.[139]

Cioslowski and Mixon[140] proposed a definition of covalent bond indices, n_{CM}, which is not directly related to the basis set: They divided the space into basins following the procedure of Bader to identify a unique volume with an "atom" (see the previous section). For a basin Ω_A and spin−orbitals $\phi_i(\mathbf{r})$, the element of the basin overlap matrix is given by

$$\langle i|j\rangle = \int_{\Omega_A} \phi_i^*(\mathbf{r})\phi_j(\mathbf{r})\, d\mathbf{r} \quad (11)$$

They argued that bond orders would be best computed in a localized orbital basis, which maximizes the sum of the squared diagonal elements of each basin overlap matrix. Having obtained these localized orbitals, the bond order is computed as

$$n_{CM} = 2\sum_i \nu_i^2 \langle i|i\rangle_A \langle i|i\rangle_B \quad (12)$$

where ν_i is the occupation number of the ith natural spin−orbital. Thus, these covalent bond indices can be defined only after localized orbitals have been determined. In other words, these indices are independent of the orbital representation. This proposal is subject to particular inconveniences for delocalized systems, where a reasonable approximation for the bond order can be obtained only by averaging different resonant structures. As an example, with benzene it leads to alternating high and low π-bond orders (i.e., a Kekulé-like arrangement). A similar behavior was observed in naphthalene, anthracene, naphthacene, and pentacene.[141] Note that this definition of bond order reflects only its covalent part; thus, bonds with substantial ionic character could show values much lower than the nominal integers usually associated with chemical bonds.

Another approach is the basin−basin sharing indices, I_{AB}.[142] They are found by integrating the point−point sharing index over the volume ascribed to basins Ω_A and Ω_B. The result is that in terms of natural spin−orbitals the basin−basin sharing indices are given by

$$I_{AB} = \sum_{i,j} \sqrt{\nu_i}\, \langle i|j\rangle_A \sqrt{\nu_j}\, \langle j|i\rangle_B \quad (13)$$

These sharing indices, depending only on the one-particle density matrix, are intrinsically independent of the orbital representation.

A quantitative comparison of the covalent bond indices and the sharing indices illustrates that these two sets of indices are different.[143] For single-determinant wave functions, it has been found that the covalent bond index is two times larger than the sharing index. Recently, the degree of electron delocalization in the ylides of phosphorus[144,145] and sulfur were investigated by using the Fulton index.[146]

Wiberg noted that in some condensed aromatic systems both indices are related to the bond length.[141] He argued that σ-components of the covalent bond index change relatively little and do not correlate well with the bond lengths. In addition, the range of π-indices is large (0.21−0.59), whereas the range of σ-indices is small (0.92−0.98). These results make it clear that the bond lengths for these compounds are largely determined by the degree of π-character in the bond.

Ángyán et al.[147] derived a covalent bond order, n_A, based on the atomic overlap matrix given in eq 11, which does not depend on any particular choice of localized orbitals:

$$n_A = 2\sum_i \nu_i \nu_j \langle i|i\rangle_A \langle i|i\rangle_B \quad (14)$$

It is easy to see that the shared index is exactly half of n_A in the case of SCF wave functions, while for noninteger occupation numbers (natural orbitals), the scaling between the two indices is more complicated. In many cases, n_{CM} (eq 12) and n_A (eq 14) give similar values, but they can differ considerably for aromatic systems.[147] Kar et al. compared the performance of HF and Kohn−Sham (KS) orbitals in a study of chemical bonding on the basis of n_A.[148] The two types of orbitals predict comparable values of bond indices, valences, and related quantities not only at the equilibrium geometry of the molecules but also at other geometries.

Howard and Lamarche explored the relationship between different covalent bond order definitions and the CPDEDs.[149] They concluded that n_{CM} for a range of bond types broadly supports the Pauling relationship as a simple one-parameter description of bond order. In polar bonds, $K(\mathbf{r})$ evaluated at (3, −1) CPs correlates with n_{CM} closer than Pauling's expression. They emphasized that neither the bond length nor any single CPDED correlates with the bond order for the five bond types considered by them (C−C, C−N, C−O, C−P, and C−S bonds). These last results show that Bader's proposal of using only ρ_b seems to be restricted to the case of C−C bonds. A multiple linear relationship

$$n_{CM} = a + b\rho_b + c\lambda_3 + d(\lambda_1 + \lambda_2) \quad (15)$$

was suggested since it works for all five of these bond types. They give a simple physical interpretation: ρ_b and λ_3 measure σ character, while the curvatures perpendicular to the bond measure the degree of π character. It is expected that this relationship can help to estimate the bond order from experimental results.

Recently, Jules and Lombardi[150] suggested to generalize the Bader formula to

$$n_B = \frac{\alpha}{\sqrt{z_1 z_2}} \exp[A_{ij}(\rho_b - B_{ij})] \quad (16)$$

where z_1 and z_2 are the number of valence electrons for each atom joined by the bond, and A_{ij} and B_{ij} are

constants with indices i and j referring to the rows of the periodic table in which the considered atoms are found. To test this formula, the experimental bond orders obtained from Guggenheimer's equation[151] in conjunction with theoretical values of ρ_b were used. They claimed that this modification of Bader's proposal makes it more generally applicable and compatible with the experimental results.

Chesnut found that lone pairs could contribute about 10−15% on average to the covalent bond order. The terms lone pair and nonbonding pair are not generally equivalent to each other because lone pairs cannot be completely localized and will exhibit a presence in the bonding regions to varying degrees. For instance, in phosphine oxides this contribution is about 44% of the total covalent bond order. Even though it is not as high in the nitrogen analogues, it is large enough to lead to a triple bond description of the NO bond in $(HO)_3NO$ and F_3NO.[152]

4. Laplacian of the Electron Density

4.1. Background

The physical interpretation of the Laplacian of a scalar function was first given by Maxwell,[153] when he stated that if the value of $\rho(\mathbf{r})$ at the center $\mathbf{r}_a$ of a small sphere with radius τ is $\rho(\mathbf{r}_a)$ and if $\rho_{av}(\mathbf{r}_a)$ is the mean value for all points within this small sphere, then the following holds:

$$\rho_{av}(\mathbf{r}_a) - \rho(\mathbf{r}_a) = \frac{1}{10}\tau^2\nabla^2\rho(\mathbf{r}_a) - O(\tau^4) \quad (17)$$

In this equation, $O(\tau^4)$ denotes terms of higher order, which are usually neglected. Note that when the value of the function at a particular point is greater than the average value of the function at neighboring points, a situation that can be described as "concentration" of ρ, the Laplacian of the function at that point will be negative. Conversely, when the value of the function at a given point is less than the average value of the function at neighboring points, a situation known as "depletion", the Laplacian of the function will then be positive.

Now, the Laplacian of the charge density is defined as the sum of the three principal curvatures of the function at each point of the space, that is,

$$\nabla^2\rho(\mathbf{r}) = \frac{\partial^2\rho(\mathbf{r})}{\partial x^2} + \frac{\partial^2\rho(\mathbf{r})}{\partial y^2} + \frac{\partial^2\rho(\mathbf{r})}{\partial z^2} \quad (18)$$

which is, as indicated, also the trace of the Hessian of the density at the corresponding point.

When $\nabla^2\rho(\mathbf{r}) < 0$, the value of ρ at point $\mathbf{r}$ is greater than its average value at neighboring points, and when $\nabla^2\rho(\mathbf{r}) > 0$, the electronic charge tends to concentrate at that point. We need to emphasize that the local concentration of the electron density does mean that the absolute value is very high.

Although the properties of the Laplacian have been known for many decades, it was only in the early 1980s that the Laplacian of the charge density had been used to study chemical problems. However, in solid-state physics it was well-known that the inclusion of the Laplacian was very important to improve the basic models of Thomas, Fermi, and Dirac. Bader and Essen proposed to characterize the properties of the atomic interactions through a study of the properties of a scalar field derived from the charge density, its Laplacian distribution $\nabla^2\rho(\mathbf{r})$.[12] A complete and meticulous discussion of the Laplacian and its use in models of reactivity is given in refs 17 and 154. The discussion in this review is limited to give an overview of the Laplacian of the electron density and its application as a measure of electron delocalization.

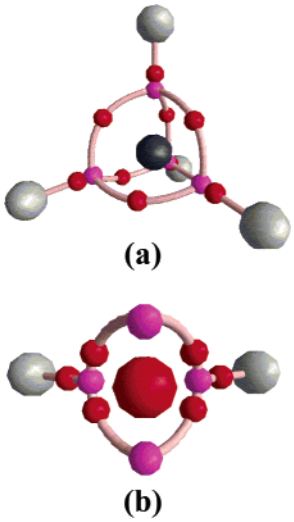

Figure 6. Valence shell charge concentration graph for (a) methane and (b) water. Purple and red spheres are the (3, −3) and (3, −1) CPs of the Laplacian of the electron density, respectively.

It is useful to define a quantity proportional to the negative of the Laplacian as

$$L(\mathbf{r}) = -\nabla^2\rho(\mathbf{r}) \quad (19)$$

consequently, the density is locally concentrated in those regions where $L(\mathbf{r}) > 0$ and locally depleted when $L(\mathbf{r}) < 0$. For a free atom, $L(\mathbf{r})$ reveals the shell structure.[155] In principle, the shell structure predicted by $L(\mathbf{r})$ is preserved when an atom is involved in a chemical reaction, but the outermost shell of charge concentration is transferred to neighboring atoms and, thus, participates in the chemical bond. We need to remark that the complexity of the topology of the Laplacian is stunning compared to that of the electron density, even for simple molecules, such as methane or water (Figure 6).[19,156,157]

The outer shell of charge concentration is called the valence shell charge concentration or simply VSCC.[17] These local charge concentrations duplicate in number, location, and size the spatially localized electron pairs of the valence shell electron pair repulsion (VSEPR) model.[158,159] Bader et al. proposed to replace the spherical surface on which the hypothetical electron pair electrons are assumed to be localized in Gillespie's model with the valence shell of charge concentration as defined, $-\nabla^2\rho(\mathbf{r})$.[154] In other words, they concluded that the Laplacian of the charge density provides the physical basis for the VSEPR model.[154,158,159]

As it will be seen in the next section, Bader and Stephens argued about the nonexistence of regions dominated by electron pairs outside of core regions or ionic systems.[160] In 1988, Bader et al. empirically found a correspondence between the local charge concentrations (CCs) in the VSCC of an atom in a molecule with the number and the spatial arrangement of the localized electron pair domains defined by the VSEPR model.[161] This paper showed that the existence of the CCs in the VSCC is the result of partial pair condensation. Furthermore, it was found that the Fermi hole obtained when the reference electron is placed at a corresponding bonded or nonbonded maximum in the VSCC is the most localized one and at least mutually overlapping. The effect is more pronounced for those geometries that maximize the separation of the electron pair domains within the model, or equivalently, maximize the separation between the CCs in the VSCC of the central atom.

The topology of the VSCC is simply and elegantly summarized by its atomic graph, the polyhedron whose vertices (V) are defined by the CCs of the (3, −3) CPs, present in its VSCC. The edges (E) connecting the CCs of the polyhedron are defined by the unique pairs of trajectories originating at the intervening (3, −1) CPs. Each of the resulting faces (F) contains a (3, +1) CP. The vertices denote the maxima in charge concentration, while the faces correspond to the regions of charge depletion in the VSCC. The atomic graph is classified by its characteristic set [V, E, F] giving the number of each type of CP and satisfying Euler's relationship $V - E + F = 2$. The topology description is the same as that applied to the density with the vertices replacing the nuclei and the edges the bond paths, etc. As recent examples have illustrated, the characteristic set of a transition metal atom M determines its donor−acceptor characteristics, as embodied in the association of a charge concentration (CC), on one reactant with a charge depletion (CD) on another. The association CC ↔ CD provides a physical complement to models based on frontier orbital arguments. In Figure 7, an atomic graph from a study of Mn complexes is reproduced to illustrate the simplicity of the presentation of this concept. A similar structure is obtained for all d^6 transition metal atoms.

In Figure 7, each green sphere represents a vertex in the atomic graph, a CC or (3, −3) CP in $L(\mathbf{r})$. The CCs are linked to one another by lines emanating from intervening (3, −1) CPs that form the Edges of the atomic graph. Each face contains a (3, +1) CP denoted by a blue sphere, a point of minimum charge concentration. The envelope map for $L(\mathbf{r}) = 17$ au displays the 12 regions of charge concentration and the six regions of charge depletion that assume the roles of the t_{2g} and e_g orbitals of crystal or ligand field theory on the Laplacian description of donor−acceptor interactions.

Bader et al. made an extensive comparison of the topologies of $L(\mathbf{r})$ and ELF($\mathbf{r}$). A large number of systems, including transition metal molecules, were tested, and it has been found that both functions have a similar topology.[94,162] This means that they are homeomorphic in terms of the number and relative arrangement of the electron domains they define. The previous ideas have been used by Bader et al. to show that the spatial distribution of the Fermi hole density provides a quantitative basis for the concept of electron delocalization commonly used throughout chemistry.[160]

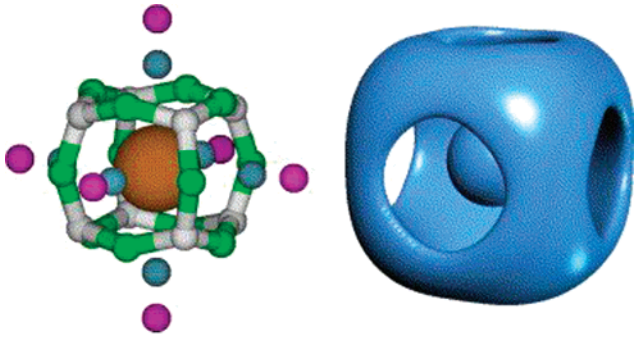

Figure 7. The trajectories linking the critical points in $L(\mathbf{r}) = -\nabla^2\rho(\mathbf{r})$ are shown on the left and envelope plot on the right for the Mn atom in $Mn(CO)_5^+$. The envelope has value of $L(\mathbf{r}) = 17$ au. The enclosed spheres indicate the inner cores. The color scheme identifying the critical points is as follows: gray (3, −3); green (3, −1); blue (3, +1); purple (3, +3). The envelope provides a striking visual display of the regions of charge concentration (CC) and charge depletion. Reprinted with permission from ref 94. Copyright 2005 Elsevier.

Recently, Bader and Heard showed the existence of a homeomorphism between the Laplacian of the electron density and the Laplacian of the conditional pair density. This homeomorphism demonstrates that the CCs displayed in $L(\mathbf{r})$ signify the presence of regions of partial pair condensation, that is, of regions with greater than average probabilities of occupation by a single pair of electrons. Thus, $L(\mathbf{r})$ provides a mapping onto $\mathscr{R}^3$ of the pairing of electrons that is determined in the six-dimensional space of the pair density; the recovery of VSEPR in the topology, for example, is an anticipated result.

4.2. Applications of the Laplacian of the Electron Density

Obviously, the major applications of the Laplacian are concerned in recovering the VSEPR model. Most of the works that have used the Laplacian distribution deal with the concentration or depletion of electronic charge, but also a few have addressed the issue of delocalization.

Gobbi and Frenking have calculated the equilibrium structures and barriers for rotation around the C−X for the allyl cations and anions, $CH_2CHXH_2^{+/-}$ (X = X, Si, Ge, Sn, Pb).[163] The allyl cations have a planar geometry and π conjugation, σ bonding, and through-space charge interactions that contribute to their stabilization and have a similar magnitude as the resonance stabilization. In contrast, the calculations suggest that there is no resonance stabilization in allyl anions, except in the parent anion, CH_2CH_2-CH_2^-.[164] The differences of the electronic structures of the C−X bonds and charge in the C−X bound upon rotation of the XH_2 group become visible by comparison of the Laplacian distribution in the π plane.

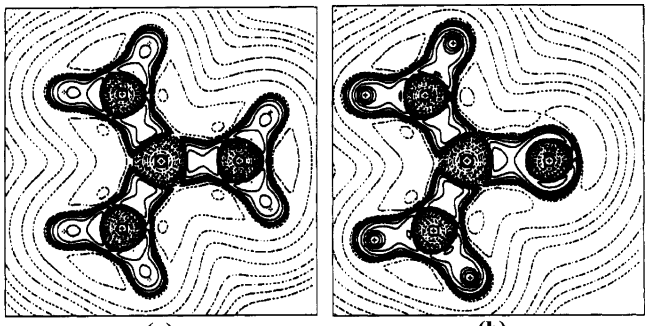

Figure 8. Contour line diagram of $L(\mathbf{r})$ of guanidinium cation for (a) the energy minimum geometry and (b) the transition state. Both are in the plane of the C and N atoms. Reprinted with permission from ref 166. Copyright 1996 American Chemical Society.

4.2.1. Y-aromaticity

Y-aromaticity suggests that acyclic conjugated species with closed shell $(4n + 2)$ π-electron configuration and branched (Y-shaped) delocalization possess "aromatic" stability. Cioslowski et al. reported results of the electronic structure of trisubstituted methanes and their congujate bases.[165] The CPDEDs of the C−H bonds poorly reflect the different origins of the substituent effects in these molecules. However, they concluded that the resonance and the inductive effects could be easily distinguished by taking into account large changes in the molecular geometries, ρ_b, and the GAPT (generalized atomic polar tensor) atomic charges. These trends are in agreement with the expectations based on the presence of Y-aromaticity in $C(CN)_3^-$ and $C(NO_2)_3^-$ anions. A similar analysis of the guanidinium cation shows that the π-electron distribution of the C−NH_2 bonds is shifted toward in the nitrogen atom (Figure 8).[166] At this atom, there is concentration in the π-electron region, while there is depletion at the carbon atom. The Laplacian for the transition state involved in the rotation shows a nonbonded CC at the nitrogen atom of the rotating amino group, which is interpreted as a lone pair. Although the resonance stabilization of the Y-conjugated species was found to be lower than generally assumed, it is an important factor for the stabilization of the molecules. In contrast, the Y-conjugated silylium cations $[Si(XH)_3]^+$ (X = O, S, Se, and Te) are strongly stabilized by π-donation from the chalcogen lone-pair electrons into the formally empty p(π) valence orbital of Si.[167]

4.2.2. Carbenes

Boehme and Frenking[168] and Heinemann et al.[169] have studied the role of π-electron delocalization in Arduengo-type carbenes and their silicon analogues. Using the thermodynamic, structural, magnetic, and electron distribution properties (in particular, the Laplacian distribution) of the above-mentioned stable cyclocarbenes and their higher homologues, they concluded that the presence of the C=C double bond in the five-membered rings gives enhanced $p_\pi-p_\pi$ "aromatic" delocalization. However, the conclusion regarding the degree of conjugation and aromaticity depends on the criteria used, being quite small according to the analysis of the electron density and the Laplacian distribution but more significant according to the energetic and the magnetic properties. All criteria agree that the aromatic character of imidazol-2-ylidenes is less pronounced compared to benzene or to the imidazolium cation. π-Electron resonance is found to be less extensive in the silylenes compared to their carbene analogues.[169]

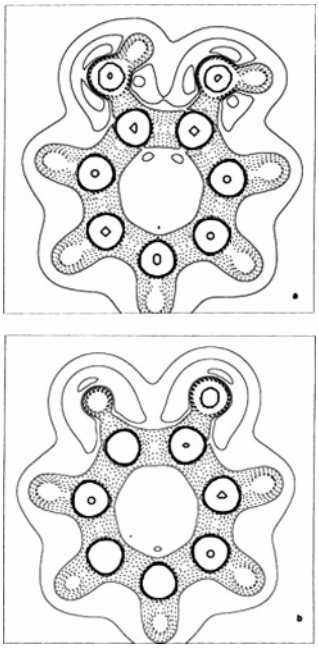

Figure 9. Contour map of the $\nabla^2\rho(\mathbf{r})$ for (a) protonated tropolone and (b) deprotonated tropolone. Positive values of $\nabla^2\rho(\mathbf{r})$ are denoted by solid lines and negative values by dashed lines. Reprinted with permission from ref 172. Copyright 1997 American Chemical Society.

Munoz-Caro et al. have studied the stability of the amide and imidic tautomers of the acetohydroxamic acid.[170] They "visualized" the conjugation using a map of the Laplacian. The existence of conjugation is translated into a smaller conformational flexibility that contributes to stabilize the intramolecular hydrogen-bonded structure.

4.2.3. Hydrogen Bonds

Garcia-Viloca et al. have discussed the low-barrier hydrogen bond in the hydrogen maleate anion.[171] The analysis of the Laplacian shows that each hydrogen bond involves a covalent interaction with the donor atom and an electrostatic interaction with the acceptor atom, except for the intramolecular proton-transfer transition state in the maleic monoanion, where both interactions are covalent. This result is in agreement with the assumption of Gilli et al.[15] that the degree of covalency increases with the shortening of the donor−acceptor distance and that in very short hydrogen bonds both O−H become essentially covalent.

Mo et al. provided experimental and theoretical information regarding the intrinsic basicity and acidity of tropolone (Figure 9).[172] The bonds, which were formally single bonds in the neutral form, increase their ellipticity upon protonation due to their higher π character. On the other hand, those that

were formally double bonds in the neutral have a smaller ellipticity in the protonated form. This is also mirrored in the characteristics of $\nabla^2\rho(\mathbf{r})$ of the charge density (see Figure 9), which clearly shows the highly delocalized nature of its charge distribution.

5. The Fermi Hole

5.1. Loge Theory

In 1955, Daudel and co-workers developed the loge theory to understand the electron pair concept.[173] In this approach, localized groups of electrons were formed by finding a separation of real space of a molecule into loges. In 1971, the loge model was rewritten in terms of Shannon's information theory. Here, the space was decomposed into regions, and these regions are formed in such way that the "missing information function",

$$I = \sum_n P_n(\Omega) \ln P_n(\Omega) \tag{20}$$

is minimized.[174] In eq 20, $P_n(\Omega)$ denotes the probability that n electrons occupy the loge. The calculation of P_n requires specialized numerical techniques, and no real applications were made until 1974, when Daudel et al. studied small molecules, including LiH, BeH, BH, and BeH_2.[175] However, the limitations of the model were evident when it was applied to larger and nonionic systems. They showed that the behavior of the missing information function was mimicked by fluctuations in the average population of the loge. The fluctuation in the population of a loge Ω is defined as[175]

$$\Lambda(\Omega) = \sum_{n=0}^{N} n^2 P_n(\Omega) - \{\sum_{i=0}^{N} n P_n(\Omega)^2\} = N^2(\Omega) - N(\Omega)^2 \tag{21}$$

where $N(\Omega)$ is the average population of the loge and $N^2(\Omega)$ is the average of the square of the number of particles. Bader and Stephens showed that while the computation of the missing information function requires the full many-particle density matrix, $\Lambda(\Omega)$ is conveniently accessible through the pair density.[176] This electron localization approach could be successfully applied for core regions and small ionic systems but not for polar or covalently bonded molecules. The reason is that the valence electron pairs in covalent molecules are so strongly intercorrelated that the localized pair model does not give an appropriate description.[160] Levy made an attempt to identify chemical bonds with the regions of minimum fluctuation of the electron pair.[177] However, the absence of spatially localized electron pairs, given by $\Lambda(\Omega)$, motivated the preliminary conclusion to drop this model. Nevertheless, the paper of Bader and Stephens demonstrated that the physical requirement for the spatial localization of electrons is the corresponding localization of the Fermi hole correlation.[160] The formation of α and β pairs is a consequence of the antisymmetrization requirement imposed on the wave function by the Pauli exclusion principle. In 1954, Lennard-Jones stated that "Electrons of like spin tend to avoid each other. This effect is more powerful, much more powerful than that of the electrostatic forces. It does more to determine the properties and shapes of molecules than any other single factor. It is the exclusion principle which plays dominant role in chemistry".[178−180] This exclusion is a result of the Fermi hole, which determines the difference between the correlated and uncorrelated pair densities for same spin electrons.[181,182] Lennard-Jones's work was unfortunately overshadowed by improperly ascribing localization to the form of localized orbitals, orbitals that originated from his own work in developing "equivalent orbitals".[178−180]

5.2. The Fermi Hole and Electron Delocalization

In 1934, Wigner and Seitz coined the term "Fermi hole": "...there is a hole in the otherwise uniform electron fluid around every electron because the probability of two electrons having parallel spin being very near is very small. We shall call this Fermi hole".[183] Salem made perhaps the first link between the Fermi hole and electron delocalization in chemistry: "The square of the bond order between atoms r and s represent the extent of the total correlation between two electron with parallel spin, one at r, the other at s".[184]

Let us start with the definition of the spinless second-order density matrix, which is given by

$$P_2(\mathbf{r}_1',\mathbf{r}_2';\mathbf{r}_1,\mathbf{r}_2) = \frac{N(N-1)}{2}\int \Psi^*(\mathbf{r}_1',\mathbf{r}_2',\mathbf{r}_3,...,\mathbf{r}_N)\Psi(\mathbf{r}_1,\mathbf{r}_2,...,\mathbf{r}_N)\, d\mathbf{r}_3\, d\mathbf{r}_4 \ldots d\mathbf{r}_N \tag{22}$$

The diagonal elements of P_2 are the two-particle density matrix, also called the pair density function, which one writes conveniently as

$$P_2(\mathbf{r}_1,\mathbf{r}_2) = P_2(\mathbf{r}_1,\mathbf{r}_2;\mathbf{r}_1,\mathbf{r}_2) \tag{23}$$

This function is proportional to the probability of finding simultaneously one electron at position $\mathbf{r}_1$ and another one at $\mathbf{r}_2$. Now, the first-order matrix can be expressed in terms of P_2 as

$$P_1(\mathbf{r}_1';\mathbf{r}_1) = \frac{2}{N-1}\int P_2(\mathbf{r}_1',\mathbf{r}_2;\mathbf{r}_1,\mathbf{r}_2)\, d\mathbf{r}_2 \tag{24}$$

where the diagonal elements of the first-order density matrix define the charge density:[181]

$$\rho(\mathbf{r}) = P_1(\mathbf{r},\mathbf{r}) \tag{25}$$

In an independent particle situation, the pair density is given by

$$P_2(\mathbf{r}_1,\mathbf{r}_2) = \frac{1}{2}\rho(\mathbf{r}_1)\rho(\mathbf{r}_2) \tag{26}$$

where the factor $^1/_2$ avoids counting the same pair twice. More generally, since the electrons are not independent particles, it is necessary to add a term to the former expression to properly take into account

the correlation existing between the electrons, namely,

$$P_2(\mathbf{r}_1,\mathbf{r}_2) = \frac{1}{2}[\rho(\mathbf{r}_1)\rho(\mathbf{r}_2) + P_{XC}(\mathbf{r}_1,\mathbf{r}_2)] \quad (27)$$

The term $P_{XC}(\mathbf{r}_1,\mathbf{r}_2)$ contains all the information related to the quantum interaction among the electrons and measures the correlation of electrons. Since the charge density and the pair density are normalized to the number of electrons N and the number of distinct electron pairs, $N(N-1)/2$, respectively, one can easily establish that

$$\int\int P_{XC}\, d\mathbf{r}_1\, d\mathbf{r}_2 = -N \quad (28)$$

For the sake of clarity, in the previous lines we have used the spinless version of the density matrices. However, when spin is taken into consideration, the corresponding holes (Fermi and Coulomb) are associated with spins σ and σ'

$$h^{\sigma\sigma'}(\mathbf{r}_1,\mathbf{r}_2) = \frac{P_{XC}^{\sigma\sigma'}(\mathbf{r}_1,\mathbf{r}_2)}{\rho^{\sigma}(\mathbf{r}_1)} = \frac{2P_2^{\sigma\sigma'}(\mathbf{r}_1,\mathbf{r}_2)}{\rho^{\sigma}(\mathbf{r}_1)} - \rho^{\sigma'}(\mathbf{r}_2) \quad (29)$$

where $\sigma = (+1/2, -1/2)$ are the spin coordinates.

For electrons with the same spin, eq 27 can be rewritten as

$$P_2^{\sigma\sigma}(\mathbf{r}_1,\mathbf{r}_2) = \frac{1}{2}\rho^{\sigma}(\mathbf{r}_1)[\rho^{\sigma}(\mathbf{r}_2) + h^{\sigma\sigma}(\mathbf{r}_1,\mathbf{r}_2)] \quad (30)$$

and it follows the very important sum rule

$$\int h^{\sigma\sigma}(\mathbf{r}_1,\mathbf{r}_2)\, d\mathbf{r}_2 = -1 \quad (31)$$

which must hold for any value of $\mathbf{r}_1$. This corresponds to the removal of one electronic charge of spin σ. Furthermore, when $\mathbf{r}_1 = \mathbf{r}_2$, eq 29 reduces to

$$h^{\sigma\sigma}(\mathbf{r}_2,\mathbf{r}_2) = -\rho^{\sigma}(\mathbf{r}_2) \quad (32)$$

ensuring the complete removal of all like-spin electrons in the position of the reference electron. Pictorially, it may be viewed as a description of how the density of an electron of given spin, the so-called reference electron, is spread out in space, thereby excluding the presence of an identical amount of same spin density.[185] An electron pair is spatially localized if the total degree of exclusion is preserved for the motion of a pair of reference electrons over the region of exclusion. This approach leads to complete localization only for core electrons and ionic systems. For valence electrons in general, the hole is delocalized and the magnitude of its density is less than the same-spin electron density for positions different from the coordinates of the reference electron. Bader emphasized that any physical measure of electron localization or delocalization is determined by the corresponding localization or delocalization of the Fermi hole.[162]

If one uses a given partitioning of the real space in a set of disjointed regions (basins), $\{\Omega_A\}$, it is possible to propose a measure of the total correlation for electrons contained within that region, and a qualitative so-called localization index $\lambda(A)$ can be calculated as

$$\lambda(A) = -\int_{\Omega_A} P_{XC}(\mathbf{r}_1,\mathbf{r}_2)\, d\mathbf{r}_1\, d\mathbf{r}_2 \quad (33)$$

while a delocalization index between a pair of basins, $\delta(A,B)$, can be obtained by integrating two electron coordinates in $P_{XC}(\mathbf{r}_1,\mathbf{r}_2)$ over regions Ω_A and Ω_B, respectively:

$$\delta(A,B) = -\int_{\Omega_A}\int_{\Omega_B} P_{XC}(\mathbf{r}_1,\mathbf{r}_2)\, d\mathbf{r}_1\, d\mathbf{r}_2 - \int_{\Omega_B}\int_{\Omega_A} P_{XC}(\mathbf{r}_1,\mathbf{r}_2)\, d\mathbf{r}_1\, d\mathbf{r}_2 = -2\int_{\Omega_A}\int_{\Omega_B} P_{XC}(\mathbf{r}_1,\mathbf{r}_2)\, d\mathbf{r}_1\, d\mathbf{r}_2 \quad (34)$$

$\lambda(A)$ gives the number of electrons that are localized in Ω_A. When an atom is fully linked by closed-shell interactions with its neighbors, $\lambda(A)$ should approach to the number of the electrons in Ω_A, N_A. This case corresponds to an ideal situation where there is no exchange or correlation between electrons in Ω_A and electrons in other basins. In real systems, there is always a degree of electron delocalization between pairs of neighboring atoms and maximal electron delocalization is present in open-shell (covalent) homonuclear interactions. Thus, for a pair of electrons shared between two identical atoms, the maximal possible delocalization corresponds to $\delta(A,A') = 1$, with $\lambda(A) = \lambda(A') = 0.5$.[186] Note that these indices are an integral part and a consequence of the conditional pair density.

Because of the normalization condition of the exchange-correlation density, the summation of all $\lambda(A)$ and $\delta(A,B)$ (the latter divided by 2) in a molecule gives its total number of electrons (N):

$$\sum_{\Omega_A}\left(\lambda(A) + \frac{1}{2}\sum_{\Omega_B\neq\Omega_A}\delta(A,B)\right) = N \quad (35)$$

The eqs 33−35 are general and can be used at any level of theory if the first- and second-order density functions are known. At the HF level, localization and delocalization indices simply can be calculated as given in the following expressions:

$$\lambda(A) = -\sum_{i,j}(S_{ij}(A)^2) \quad (36)$$

$$\delta(A,B) = -2\sum_{i,j} S_{ij}(A)S_{ij}(B) \quad (37)$$

Here, $S_{ij}(A)$ denotes the overlap integral of the molecular orbitals i and j within the region Ω_A.

Note that at the HF level, the delocalization index (eq 37) is equivalent to the Fulton index[142] (eq 13). Bader stated that "Fulton and Angyan, Loos and Mayer have defined bond orders which, at the Hartree−Fock level of theory, yield values identical to those obtained using $\delta(A,B)$ but do so without reference to the underlying physics. That is, they do not relate their definitions to the properties of the density of the Fermi hole".[187]

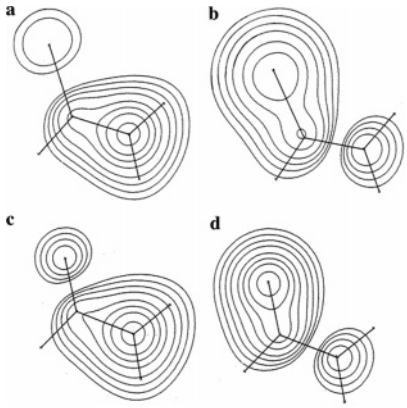

Figure 10. Contour diagrams that graphically display the extent of the Fermi holes of the π density in thioformamide (a,b) and formamide (c,d). The amid group is always on the right-hand side of the molecule. The reference electron is placed above S (b) and O (d) and above the N atom (a,c). Reprinted with permission from ref 192. Copyright 1996 American Chemical Society.

Finally, it is worth noting that the definition of delocalization index can be generalized to study multicenter bonding.[148,188−190] For instance, the three-center bonding delocalization index can be computed at the HF level as

$$\delta(\mathrm{A,B,C}) = 2\sum_{i,j,k} S_{ij}(\mathrm{A})S_{jk}(\mathrm{B})S_{ki}(\mathrm{C}) \qquad (38)$$

However, this generalization to post-HF theory is mathematically challenging, because it requires the computation of correlated higher-order densities.

5.3. Applications of the Fermi Hole Analysis

The great majority of applications concerned with the analysis of the Fermi hole were published in the past decade. However, the first application can be traced as far back as 1963, and it was presented by Bent, who studied the structure and bonding of nitrogen oxide dimers.[191] In 1996, Laidig and Cameron used the Fermi hole analysis to show that there is little delocalization of the π charge density from nitrogen to sulfur in thioformamide.[192] In Figure 10, representative π density Fermi holes of planar formamide and thioformamide are illustrated. From these pictures, one obtains the qualitative result that the π electrons are largely localized in both the planar formamide and thioformamide, independent of whether the reference electron is placed at the N or at the O (S) atom. Indeed, the π density is localized within the basin of the N, O, or S atom, and only a small fraction of the π density is found to be delocalized from one end of the molecule to the other. The larger barrier of rotation in thioamides and the negligible delocalization of π charge from nitrogen to sulfur disagrees with the resonance model but is consistent with a model in which (thio)amides behave as "(thio)formylamines".

In 1996, Bader et al. proposed that the spatial distribution of the Fermi correlation can be used to provide a quantitative method for the evaluation of electron delocalization.[193] The atomic delocalization

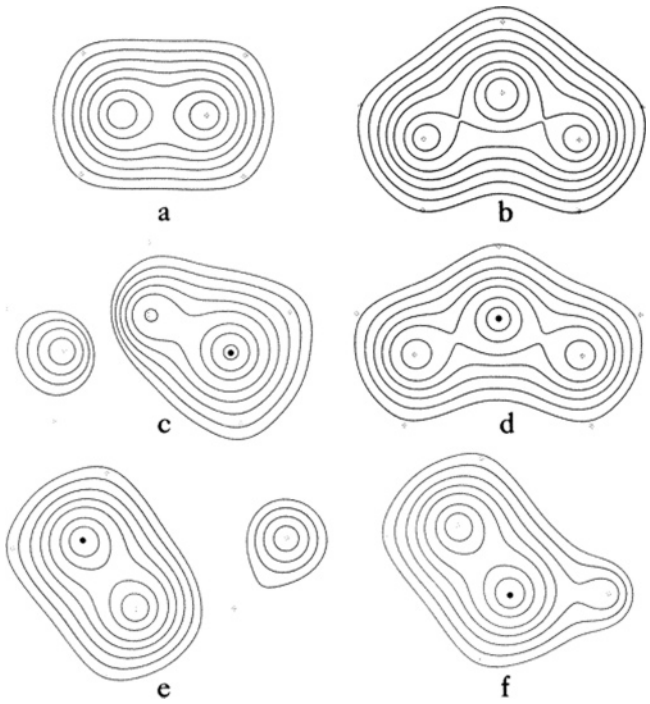

Figure 11. Contour maps of the Fermi hole density of π-electron pairs. The contour maps are given for the π_α electron in ethene (a) and in the allyl cation (b). For the allyl anion, two positions of the reference electron are shown, at a terminating carbon (c) and at the central carbon (d), and for butadiene, again with the reference electron at a primary carbon (e) and at a secondary position (f). The values of the Fermi hole density at the positions of the reference electron are 0.095 in panel c, 0.060 in panel d, 0.071 in panel e, and 0.071 in panel f. Reprinted with permission from ref 193. Copyright 1996 American Chemical Society.

patterns of the Fermi hole have been found to recover the resonance structures of the molecule, as they correspond to different possible spin-pairings. In a molecule with a single π electron or a single α, β pair, such as ethene or the allyl cation, the Fermi hole density reduces to the density of the single π orbital, independent of the position of the reference electron (Figure 11).

In Figure 12, contour plots of the Fermi hole density are depicted for the cyclopentadienyl anion, for benzene in D_{6h} and D_{3h} symmetries, and for the tropylium cation. The extent of π-electron localization at a given carbon decreases with a decreasing atomic spin population, having its maximum value in the anion. In these symmetric cyclic molecules, significant delocalization over both neighboring atoms is observed. This π-electron delocalization increases with ring size, and therefore, the electrons are more delocalized in cyclic molecules than in acyclic ones. The π density delocalization in the tropylium cation is somewhat greater than it is in benzene, which can be rationalized by the greater spatial extent available in the seven-membered ring. In benzene, however, there is significantly greater "long-range" delocalization of the π density: a higher density is observed in the basins of the para carbons compared to those of the meta carbons. Comparing benzene with its D_{3h} Kekulé-like isomer, 1,3,5-hexatriene, the π-electron density of benzene is found to be more strongly

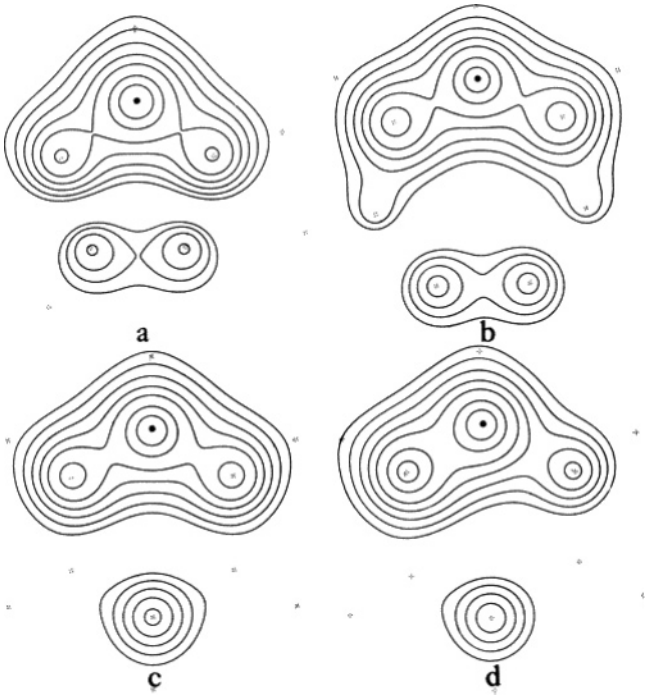

Figure 12. Contour maps of the Fermi hole density for the π_α electrons for indicated positions of the reference electron located 0.5 au above the nuclear plane. The value of the density (in au) at the position of the reference electron is given in parentheses: (a) cyclopentadienyl anion (0.080), (b) tropylium cation (0.061), (c) D_{6h} benzene (0.071), and (d) 1,3,5-hexatriene (0.071). Reprinted with permission from ref 193. Copyright 1996 American Chemical Society.

delocalized than in the Kekulé-like structure. In a figurative conclusion, we can understand the Fermi correlation as the mechanism whereby distant atoms communicate with each other.

The group of Wang used the Fermi hole and the Laplacian of the electron density to verify and understand the π-delocalization in several transition metal complexes.[194−199] In ref 195, the chemical bonds in bis(diiminosuccinonitrilo)nickel have been analyzed quantitatively in terms of topological properties of the electron density (Figure 13), which was obtained by X-ray diffraction and by theoretical calculations. The asphericity of the electron density around the Ni ion is easily accessed from the Laplacian, when a density accumulation in the d_π direction is observed, while a depletion of density along the d_σ (Ni−N) direction is found. The CPDEDs allow a classification of the bonding between Ni and the imino nitrogen atom: it is mainly a closed-shell interaction, with some covalent character. All bonds within the ligands are shared interactions, and the bond order is reflected clearly from ρ_b. The π-delocalization of the molecule is precisely indicated by ϵ and is also illustrated by the Fermi hole distribution. Apparently, the π-density is essentially distributed between the nitrilo C and N atoms and their neighbors, which indicates a localized π-bond (Figure 13b). In contrast, when the reference electron is placed on any C or N atom of the ring, the Fermi hole density is spread out over all ring atoms (Figure 13a). The Fermi hole analysis reveals the fact that the iminosuccinonitrilo ligands have a completely delocalized system of π-electrons and are monoanionic moieties.

The topological analysis of the experimental and theoretical electron density of 1,3,5,7-tetra-*tert*-butyl-*s*-indecene was performed by the same group,[200] and the Fermi hole analysis confirms the electron delocalization in *s*-indecene. They calculated the Fermi hole functions with DFT putting the reference elec-

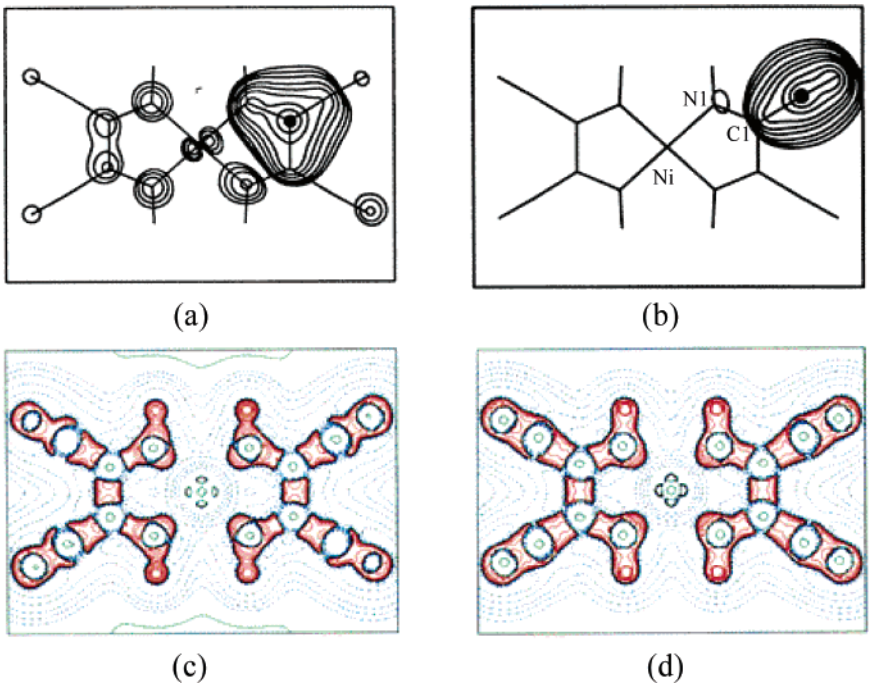

Figure 13. Fermi hole functions at the plane of 0.7 au above the molecular plane with the reference electron placed on this plane at (a) N1 and (b) Cl in bis(diiminosuccinonitrilo)nickel complex. A negative Laplacian is obtained at the molecular plane (c,d), where panel c is from experiment and panel d is from calculation. Contours are $2^i \times 10^j$ e Å^{-5} (i = 1, 2, and 3), where $j = -1$, 0, and 1. The solid red line indicates positive, the broken blue line negative, and the green line zero values. Reprinted with permission from ref 195. Copyright 1996 American Chemical Society.

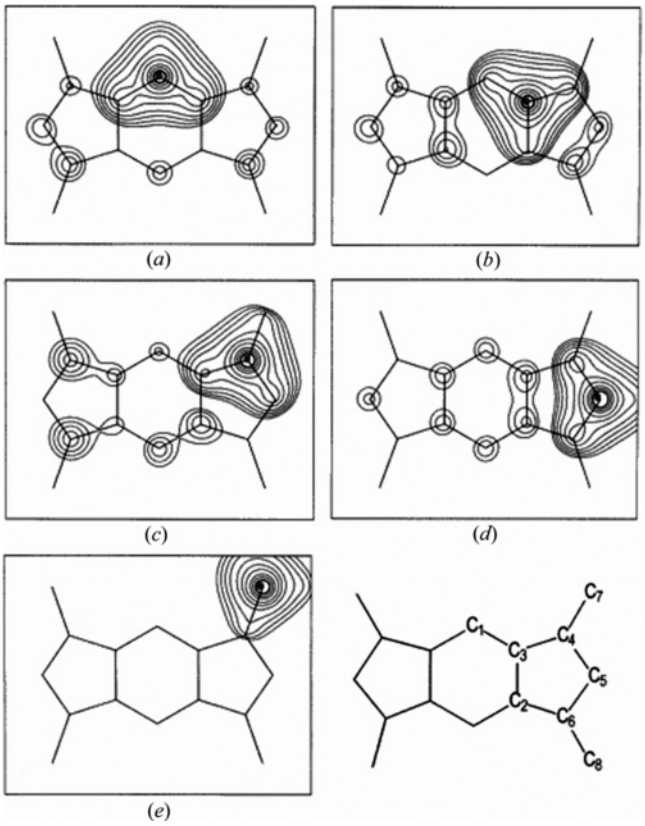

Figure 14. Fermi hole function of 1,3,5,7-tetra-*tert*-butyl-*s*-indecene calculated by DFT in the plane 0.5 Å above the ring with the reference electron (●) placed in this plane above (a) C1, (b) C3, (c) C4, (d) C5, and (e) C7. Reprinted with permission from ref 200 (http://journals.iucr.org/). Copyright 2004 International Union of Crystallography.

tron 0.5 Å above the ring plane of *s*-indacene at various C-atom sites. The Fermi hole density is distributed over the entire framework of carbon rings when the reference electron is located at either of the six-membered rings (Figure 14). Obviously, the C atom of the *tert*-butyl group does not participate in this π delocalization as evidenced in Figure 14.

5.4. The Domain-Averaged Fermi Hole

Ponec's group has defined the domain-averaged Fermi hole, $g_\Omega^A(\mathbf{r}_1)$, as the Fermi hole associated with Ω in the molecule A:[201−203]

$$g_\Omega^A(\mathbf{r}_1) = N_\Omega \rho_A(\mathbf{r}_1) - 2\int_\Omega P_2(\mathbf{r}_1,\mathbf{r}_2)\, d\mathbf{r}_2 \quad (39)$$

where N_Ω is the mean number of electrons in the region Ω and $P_2(\mathbf{r}_1,\mathbf{r}_2)$ is the pair density. Note that the Fermi hole is closely related to P_{XC} and λ(A).

Evidently, the form of $g_\Omega^A(\mathbf{r}_1)$ depends on the particular form of the region Ω. This correspondence is generally justified because $g_\Omega^A(\mathbf{r}_1)$ is often well *localized* in the same region over which the averaging was performed. This intuitive association of $g_\Omega^A(\mathbf{r}_1)$ with the fragment electron density is depicted in Figure 15. It displays the isosurface of the domain-averaged Fermi hole of benzoic acid, for which the COOH group was chosen as the region Ω over which the averaging was performed.[204]

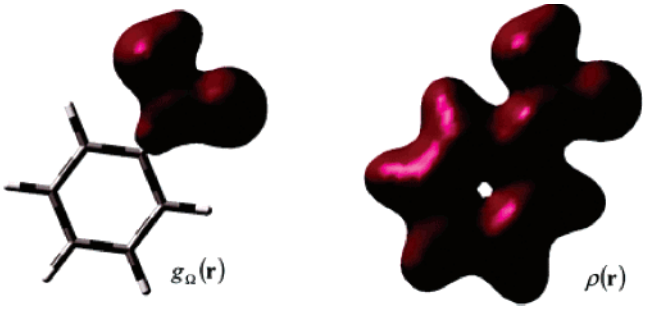

Figure 15. Comparison of a density contours of benzoic acid for $g_\Omega^A(\mathbf{r}_1)$, Ω = COOH, and $\rho(\mathbf{r})$. Both isosurfaces correspond to the same value, 0.03 e/au^3. Reprinted with permission from ref 204. Copyright 2003 American Chemical Society.

Ponec stated that the analysis of $g_\Omega^A(\mathbf{r}_1)$ yields information about the valence state of the atom in the molecule. Similarly, it is also possible to analyze the holes averaged over more complex domains, which are formed by several atomic subdomains that correspond, for example, to a functional group. In such a case, this function yields information about the chemical bonds and electron pairs within the fragment as well as about the bonding interactions of the fragment with the rest of the molecule. With use of this approach, several molecules have been studied.[203,205−211] For instance, the nature of bonding in SF_6 and CLi_6 was analyzed by Ponec and Xirones.[209] It has been shown that, although the molecule of SF_6 does not satisfy the charge criterion of hypervalence, the actual picture of bonding is consistent with the traditional hypervalent model assuming the existence of six localized albeit polar SF bonds around the central atom. On the other hand, while a charge criterion will label the CLi_6 molecule as an ideal candidate for hypervalency, the picture provided by $g_\Omega^A(\mathbf{r}_1)$ is considerably different, and it can be better characterized by the term hypercoordination.

5.5. Delocalization Indices

The delocalization index (DI) is a measure of the number of electrons that are shared or exchanged between Ω_A and Ω_B.[186] One expects that it will vary continuously along the sequence "covalent" → "polar" → "ionic". The localization of the electrons within the parallel basins increases proportional to the interatomic charge transfer, causing a reduction in δ(A,B).[186] In H_2, δ(H,H) = 1, meaning that an electron pair is equally shared between the two hydrogen atoms. The HF delocalization values for the C−C bonds in ethane and ethylene are 1.0 and 1.9. However, when the two centers A and B differ in electronegativity, the shared electron pairs contribute unequally to δ(A,B). Further examples are N_2 and CO, for which δ(N,N) = 3.04 compared to only δ(C,O) = 1.6 in polar CO. In the limit of purely ionic bonding, the electron pair would be fully localized on the anion and the DI would tend toward zero. This is the case of LiF, where δ(Li,F) = 0.19.[186]

Fradera et al. noted that the introduction of Coulomb correlation takes one beyond the Lewis model.[186] It reduces the DIs for shared interactions,

and fewer electron pairs are shared in homopolar interactions than predicted by the Lewis model at the correlated level. Thus, the values at the HF level represent upper bounds to the number of Lewis electron pairs shared between equivalent atoms. The effect of Coulomb correlation on the pairing indices is minimal for ionic molecules because of the high degree of localization of the density within each basin. In general, a proper account of the electron correlation is important for a correct description of the atomic interactions if one is interested in studying electron localization and delocalization.[212] HF overestimates strongly the interatomic delocalization between bonded atoms with open-shell interactions compared to the configuration interaction (CI) method. However, HF gives qualitatively good results for closed-shell or nonbonded interactions. The differences between HF and CI results can be attributed to the effects of Coulomb electron correlation in the one-electron density. Recently, Wang et al. proposed a practical and efficient implementation to evaluate the DIs at post-HF levels.[213] They tested a large set of molecules and compared the delocalization indices obtained from HF and conventional correlation methods (MP2, MP4, CISD, QCISD) and observed the same tendency: the DIs are similar only for molecules with large charge separations (ionic bonding).[214]

Delocalization indices cannot be calculated exactly in the framework of Kohn−Sham density functional theory (KS-DFT), where the electron-pair density is not defined. Therefore, the use of the HF formalism with the KS orbitals is the only practical way to obtain localization and delocalization indices within KS-DFT. However, it is important to remark that Coulomb electron correlation is not fully considered in these calculations.[215] In general, it has been found that KS-DFT DIs (with the B3LYP functional) are larger than those obtained with the HF method. Thus, despite the fact that the DFT one-electron density is clearly superior to HF, the DFT two-electron density calculated with KS orbitals is worse than using the HF orbitals.[215,216]

Fradera and Sola have determined localization and delocalization indices at the UHF and ROHF levels of theory to analyze the electron-pair structures of some representative doublet and triplet simple radicals.[217] In general, interatomic delocalization between bonded atoms is tightly related to the order and polarity of the bond. Atomic populations reveal that, in most cases, the spin density is preferentially localized into one of the atomic basins. This trend is more evident in molecules such as O_2, where the unpaired α electrons are located in antibonding orbitals. At the ROHF and UHF levels, this analysis is generally in qualitative agreement with the predictions of the Lewis model.[217]

Bader and Bayles showed that the transferability of the degree of localization of the electrons to a given group is a result of the conservation of the delocalization of its electrons over the remaining groups in the molecule.[218]

Poater et al. studied the effects of solvation in the electronic and molecular structure of several systems,

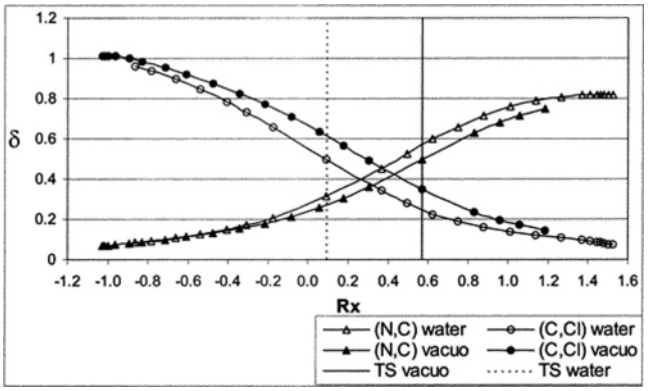

Figure 16. Evolution of the values of delocalization indices along the intrinsic reaction path of the $CH_3Cl + NH_3 \rightarrow Cl^- + CH_3NH_3^+$ Menshutkin reaction, both in vacuo and in a continuum representation of the solvent (water), calculated at the HF/6-31++G* level of theory. Negative and positive values of the distinguished reaction coordinate, defined as $R_x = r_{CCl} - r_{CN}$, correspond to reactant and product, respectively. Reprinted with permission from ref 219. Copyright 2001 American Chemical Society.

including neutral, anionic, and cationic species, as well as the stationary points of the Menshutkin reaction between methyl chloride and ammonia.[219] They concluded that localization and delocalization indices reflect the effects of solvation on the one- and two-electron density. For the Menshutkin reaction, the analysis of the DIs allows one to follow in detail the changes in electron pair structure that take place along the reaction (Figure 16).

Electronic localization and delocalization indices have also been used to study the electron-pair reorganization that takes place in five chemical reactions: two intramolecular rearrangements, a nucleophilic substitution, an electrophilic addition, and a Diels−Alder cycloaddition.[215] The λ and δ indices reflect the gradual electronic changes taking place along a reaction path. For several reactions, the main changes in the charge density topology and in electron pairing take place at different points of the intrinsic reaction path (IRC). Thus, λ and δ indices provide useful information that cannot be obtained from a simple charge density analysis. In particular, the delocalization indices in the transition state of concerted Diels−Alder reaction are able to detect the aromaticity of this structure and reveal that there is not a simple correlation between interatomic distance and electron delocalization.

Mosquera and co-workers calculated the DIs for the neutral and protonated forms of uracil and cytosine.[220] They observed that while the evolution of the chemical descriptors after the protonation can be partially explained by using resonance forms, the Bader charges and delocalization indices are *inconsistent* with those forms. They also noted that atomic populations and DIs can be related to the acidic character of phenol derivatives,[221] although these properties cannot be related to predictions provided by the resonance model.

Linear carbon chains containing sulfur C_nS (n = 1−6), which are of interest for astrochemistry and astrophysics, were examined by Perez-Juste.[222] Most of the electron delocalization takes place in the π

system, but there is also a significant contribution of σ delocalization.

The DIs associated with an intermolecular hydrogen bond depend on the interaction energy of the complex, but also on the nature of the H-donor and acceptor atoms.[223] The intermolecular DI appears to be strongly correlated to the orbital interaction energy term as obtained from an energy decomposition scheme based on conceptual Kohn−Sham theory. Both, the topological analysis of the electron density and the energy decomposition analysis allow for a characterization of the hydrogen bonds in these complexes. Daza et al. analyzed structures and bonding of $H_2O_2\cdots X$ complexes ($X = NO^+$, CN^-, HCN, HNC, and CO).[224] Hydrogen bonding is formed mainly by electrostatic interactions with a small electron delocalization δ(X,H) between the hydrogen bonded atoms. There is also a decrease in the δ(O,H) and δ-(O,O) values with the complexation, compared to the hydrogen peroxide monomer.

Chesnut has calculated the DIs and ELF(**r**) for a variety of P−O bonds of several molecules with the aim to characterize the phosphoryl bond.[225] One cannot distinguish the phosphoryl bond from a conventional PO double bond by comparing bond distances. Based on the PO bond in HPO having a reference DI of 2.0, the phosphoryl bond has a DI of about 1.3. A high degree of back-bonding contributes to the DI, providing a stronger character than a single bond and its concomitant shortening of the bond distance. A similar scheme has been applied to sulfuryl, thiophosphoryl,[226−228] and bicyclic sulfoxide derivatives.[229]

Molina et al. studied the nature of the bonding between the gallium atoms in bent $[HGa-GaH]^{2-}$.[187] The central question is how many Lewis electron pairs are shared between the two Ga atoms. The value of δ(Ga−Ga) for the dianion equals 1.7 for the HF optimized geometry and increases to 2.0 for the experimental Ga−Ga distance. Since the HF value represents an upper limit to the number of the shared pairs of electrons, there is no Ga−Ga triple bond in $[HGa-GaH]^{2-}$. This conclusion is in accord with the properties exhibited by the Laplacian of the density and by ELF(**r**). Chemical bonding in Si_2H_2[230] and Ga_2H_2[231] systems were studied by Chesnut. He found that, in general, ratios of basin populations, delocalization indices, and ELF(**r**) suggest a single and a triple bond in Si_2H_2 and Ga_2H_2, respectively.

Ylides are compounds in which an anionic site Y^- (originally on C, but now also including other atoms) is attached directly to a heteroatom X^+ (usually N, P, or S), carrying a formal positive charge. They are thus 1,2-dipolar species of the type $R_mX^+-Y^-R_n$ (Scheme 11). Dobado et al. have calculated the

Scheme 11

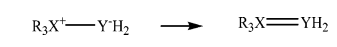

delocalization indices in a series of ylides and concluded that when X is a highly electronegative atom, the C−X bond is weaker than a single bond, due to electrostatic repulsion. In contrast, when the X atom has an electronegativity similar to carbon, a polar interaction results, which is governed mainly by

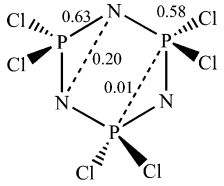

Figure 17. Bond delocalization indices obtained by a HF/6-31G** calculation of hexachlorocyclotriphosphazene. All values are given in atomic units. Reprinted with permission from ref 234. Copyright 2001 American Chemical Society.

electrostatic interactions with a small contribution of negative hyperconjugation.[232] However, several structural and electronic effects of ylides showed that some increases in the bond multiplicity are not reflected by the DIs.[233]

HF results for hexachlorocyclotriphosphazene show that the N−P and P−Cl interactions have a significant ionic character (see Figure 17).[234] Luana et al. comment that the sharing of electron pairs is not limited to those atoms directly linked in the molecular graph. For instance, the nitrogen atoms in the phosphazene ring have a nonnegligible $\delta(N,N) = 0.20$, even if they are not linked by a bond path. Since a nonvanishing DI exists between every pair of atoms in a molecule, in general, it is inappropriate to identify it with a bond order in the general case.[187]

Dobado et al. have also studied multiple bonding in a series of Ti(IV) and Ge(IV) methoxides.[235] Comparison between both series of complexes shows the existence of multiple bonding in the Ti(IV) compounds. In contrast, the Ge compounds present only Ge−O single bonds. Since δ(Ti,O) values are considerably higher than the corresponding δ(Ge,O) values (ca. 1.0 and 0.7 electron pair, respectively) and taking into account the very polarized nature of the bonds (the formal δ value for a pure ionic bond is zero), the values are consistent with Ti−O multiple bonds and with noticeable covalent character.

Poater et al. studied the properties of Fischer-type chromium−carbene complexes (Scheme 12) in terms

Scheme 12

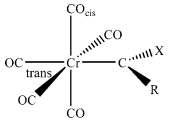

of the DIs.[236] They paid special attention to the Cr=C and C−X bonds, and the effect of the X and R substituents on the character of these bonds (X = H, OH, OCH_3, NH_2, and $NHCH_3$ and R = H, CH_3, $CH=CH_2$, Ph, and C≡CH). They found that the π-donor character of the substituent X has the largest impact on the electron delocalization between the Cr, C, and X atoms. Moreover, the fact that the DI between the nonbonded Cr and X atoms is relatively high in most of these carbenes gives some support to the concept of a three-center bonding interaction in the Cr=C−X moiety.

In 2002, the electron density distribution in a transition-metal dimer containing a semibridging carbonyl has been determined through experimental X-ray diffraction and quantum chemical computa-

tions by Macchi et al.[237] The smooth continuum of conformations observed in the solid state has been explained in terms of the mutual interplay of direct M−M and M−CO and indirect M···M and M···C interactions, which were characterized by the delocalization indices. For a terminal carbonyl in a neutral complex, δ(M,O) is about 0.15, but it increases with the negative charge of the molecule. In $[FeCo(CO)_8]^-$, the terminal carbonyls have, on average, δ(Fe,O) = 0.20 and δ(Co,O) = 0.18. It is noteworthy that for the semibridging carbonyl δ(Co,O) = 0.18 and δ(Fe,O) = 0.09, which means that the Fe−(CO) back-bonding is already quite significant, despite the long metal−carbonyl distance. This also agrees with the computed charge of the semibridging carbonyl ($q = -0.40$), which is more negative than that of a terminal CO ($Q = -0.25$). According to the above considerations, bridging carbonyls are more π-acidic than terminal ones.[237]

Recently, Cortes-Guzman and Bader have studied a series of carbonyl and cyclopentadienyl complexes.[94] The most important observation concerning the carbonyl complexes is the significant degree of delocalization between the metal and the carbon atoms with δ(M,C) values clustered around unity, indicating a close to equal sharing of one Lewis pair between M and each of the C atoms. The delocalization of the metal electrons onto the oxygens is 20% smaller. An important result is the decrease in the localization of the density of a carbon atom, from a value of λ(C) = 81% in free CO to values of ~70% in the complexes. This is not simply the effect of each carbon being in the presence of an increased number of atoms but is rather the result of the significant delocalization, that is, sharing of the density between each carbon and the metal atom. This is accompanied by a decrease of ~0.2 in the value of δ(C,O) from its uncomplexed value, which is associated with a C−O bond lengthening of 0.02 au. The metal atoms in the metallocenes extend the delocalization of the metal atom electrons onto the carbons of the cyclopentadienyl rings. The total number of electrons exchanged between M and the carbons of the rings is simply 10 × δ(M,C), which equals 1.3, 2.5, and 4.5 for the Al, Ge, and Fe complexes, respectively. The value of 4.5 for ferrocene translates into the exchange of just over two Lewis electron pairs with each ring. The values of δ(C−C) between bonded and opposite carbons in the cyclopentadienyl rings of the complexes approach the values of 1.39 and 0.13 found in the cyclopentadienyl anion, reflecting the transfer of electrons from the metal atom to the rings.

In 1998, Tomaszewski et al. synthesized an organometallic complex with a short contact between a Ti atom and a saturated carbon (Figure 18).[238] They claimed that this interaction would qualify as the first experimental example of an agostic interaction between a metal center and a saturated carbon. Later on, Bader and Matta carried out the analysis of the charge distribution in this complex,[93] finding no bond paths linking the Ti to the carbon exhibiting the short contacts. Using the DIs, they found that the delocalization between Ti and C (short contact) is minimal, equal to that found between next nearest neighbor

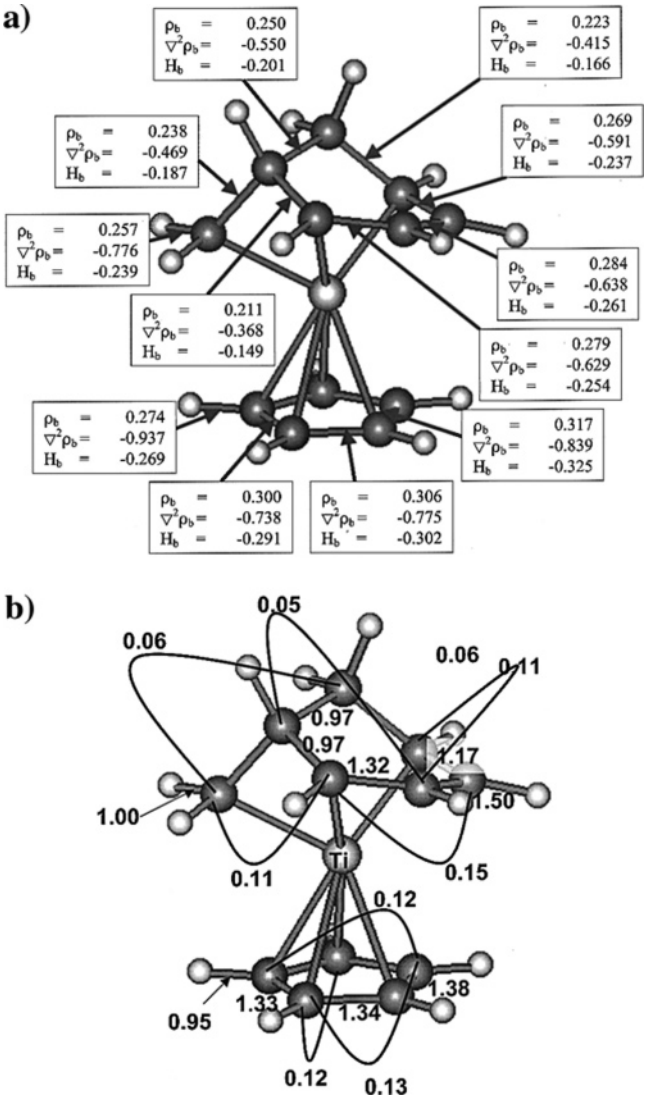

Figure 18. (a) The electron density, ρ_b, the Laplacian of the density, $\nabla^2\rho_b$, and the energy density, H_b, in au, of an organometallic complex with a short contact between a Ti atom and a saturated carbon, and (b) Hartree−Fock values of the delocalization index δ(C,C′) for neighboring (bonded) and next-nearest (NN) neighboring carbon atoms, the NN pair of atoms being linked by a curved line. Reprinted with permission from ref 93. Copyright 2001 American Chemical Society.

saturated carbon atoms (Figure 18), ruling out the experimental conclusion.

The spin−spin coupling of protons, measured by the characteristic coupling constant $J_{HH'}$ in NMR experiments, is dominated by a term proportional to the product of the electron spin densities at the two nuclei, the Fermi contact term. It was demonstrated that the DIs for the vicinal protons in ethane yield an excellent correlation with their coupling constants as a function of the torsion angle about the C−C axis, as predicted by the Karplus equation.[193] Matta et al. have used the DIs to construct a model relating $J_{HH'}$ to δ(H,H′) for hydrogen atoms bonded to different carbons in alkanes, alkenes, their cyclic congeners, and polybenzenoid hydrocarbons (Figure 19).[185] This correlation is an example of how the Fermi exchange density provides the vehicle for the transmission of information between the basins of nonbonded atoms.[185]

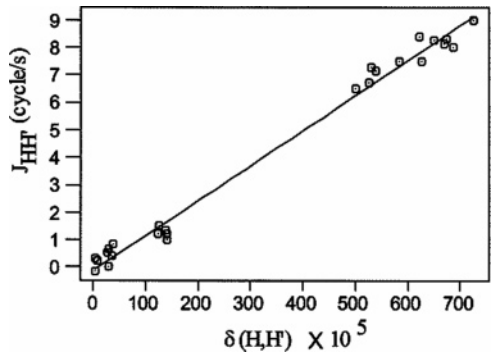

Figure 19. A scatter plot of the hydrogen−hydrogen delocalization indices, δ(H,H′), vs the proton−proton NMR spin−spin coupling expressed in cycles per second (Hz) in polybenzenoid hydrocarbons. Reprinted with permission from ref 185. Copyright 2002 American Chemical Society.

Matta and Hernández-Trujillo have investigated several correlations between the delocalization index and the CPDEDs for a series of PAHs.[239] They found an exponential relationship between the DIs and ρ_b, which could be exploited for a fast estimation of an unknown delocalization index. On the basis of these results, they defined an aromaticity index similar to the geometric HOMA index using the DI as a measure of alternation within a ring:

$$\theta = 1 - \frac{c}{n}\sqrt{\sum_{i=1}^{N}(\delta_0 - \delta_i)^2} \qquad (40)$$

In this expression, c is a constant such that $\theta = 0$ for cyclohexane, $n = 6$ for PAHs, δ_0 is a reference value, namely, the total electron delocalization of a carbon atom of benzene with all other C atoms in that molecule, and δ_i is the total electron delocalization of a carbon atom with the other carbon atoms forming a ring in a given PAH. Note that this index does not rely on the $\sigma-\pi$ separability assumption. Therefore, the annulation results in a loss of aromaticity of middle ring and increases the aromatic character of the peripheral ring.

Recently, Poater et al. have measured the electron delocalization in C_{60}.[240] They have divided C_{60} into four different layers according to the proximity of the carbon atoms to the reference atom, and the global electron DI has been calculated for each layer. They concluded that the electron charge of an atom in C_{60} is mostly delocalized into the first layer, that is, into the 13 closest atoms, enclosing two six-membered rings and two five-membered rings. When moving away from the first layer, the DIs rapidly tend toward zero. This is attributed to the fact that the electron charge of each carbon atom in C_{60} can be delocalized over more atoms than in smaller aromatic systems such as benzene or naphthalene, thus giving an unexpectedly large value for the global DI per carbon atom. However, when the electron delocalization is analyzed from a local point of view, it is seen that C_{60} has a lower delocalization and aromaticity than typical aromatic molecules because of its partial π-bond localization, which prevents the delocalization between carbon atoms in para positions.

Chesnut and Bartolloti have applied the DIs to a series of substituted cyclopentadienyl species, proving that, for a given compound, there is a good correlation between the DI of a single C−C bond and the corresponding aromatic stabilization energy (ASE) value.[241] Finally, the delocalization indices have been recently reported for pyrene,[242] twisted amides,[243] morphine,[116] and several nonclassical carbocations.[244,245]

5.6. Para Delocalization Index

Recently, the group of Sola introduced a new local aromaticity index, defined as the mean value of all DIs of para-related carbons in a given six-membered ring, the so-called para delocalization index (PDI).[246] It has been shown that there are satisfactory correlations between NICS, HOMA, and magnetic susceptibilities with PDI for a series of planar PAHs.[246] This index has been used to study the change in the local aromaticity on going from benzene to buckminsterfullerene through a series of planar and curved PAHs.[247]

The substituents attached to benzene influence weakly the π-electron delocalization in the ring, as shown by the small variation of the geometry-based index of aromaticity, HOMA, the indices based on magnetic shielding, NICS, NICS(1), and $NICS(1)_{zz}$, and the PDI.[248] The stabilization energies derived from homodesmic reaction schemes vary largely due to the imbalanced additional effects, such as strain, conjugation, repulsive interactions, etc., which contaminate the estimated ASE values. In this context, the aromatic stabilization energies do not seem to be good descriptors of the changes of π-electron delocalization in substituted benzenes. In contrast, the PDIs appear to be very successful for this purpose. The PDI correlates nicely with substituent constants.

A particular case is carbazole. Poater et al. have investigated the correlation between NICS, HOMA, and PDIs in carbazole derivatives and concluded that there is a clear divergence among the three methods used to quantify the local aromaticity.[249] Thus, one must be very cautious with the results. It is very important to warn chemists about the limitations of the different methods to analyze aromaticity.[249]

The performance of the NICS concept as a measurement of aromaticity was analyzed by Poater et al.[250] In a complete and systematic study of the local aromaticity of the six-membered rings of planar and pyramidalized pyracylene species (Figure 20), they showed that there is a small reduction of local aromaticity in the six-membered rings of pyracylene with a bending of the molecule. The slight reduction of the HOMO−LUMO gap is in line with a small decrease of global aromaticity. The ring current maps, PDIs, and HOMA indices provide analogous trends in the local aromaticity. In contrast, NICS values depend on the position where the calculation is carried out. While NICS(0) values are distorted by the bending and do not follow the trend of the other indices (and wrongly point out a large increase of aromaticity upon distortion), NICS(1), that is, NICS calculated at 1.0 bohr above the molecular plane, also

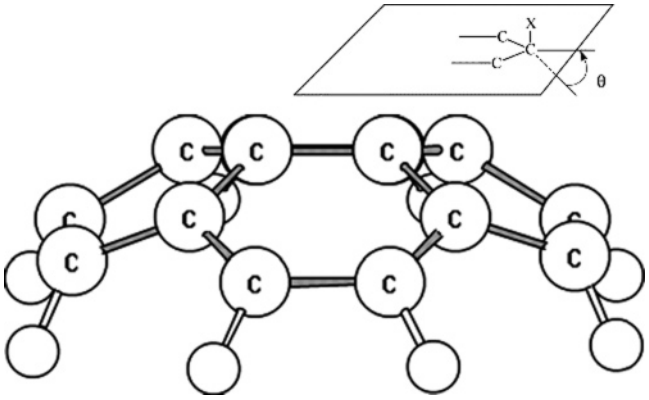

Figure 20. B3LYP/6-31G** optimized geometry for pyracylene pyramidalized by $\theta = 30°$. Reprinted with permission from ref 250. Copyright 2004 American Chemical Society.

indicates a slight decrease of aromaticity with the bending.

6. Molecular Electrostatic Potential

The molecular electrostatic potential (MEP) at any point **r** in the space around a molecule is given by

$$V(\mathbf{r}) = \sum_A \frac{Z_A}{|\mathbf{r} - \mathbf{R}_A|} - \int \frac{\rho(\mathbf{r}')}{|\mathbf{r} - \mathbf{r}'|} \mathrm{d}^3\,\mathbf{r}' \qquad (41)$$

where the first term denotes the contribution due to nuclei, $\{Z_A\}$, located at $\{\mathbf{R}_A\}$ and the second term arises due to the continuous electronic charge density distribution. This scalar field is experimentally accessible and intuitively familiar to chemists. The molecular electrostatic potential is a well-established tool for exploring molecular reactivity, intermolecular interactions, and a variety of other chemical phenomena.[251−255] Since the work of Scrocco and Tomasi,[256,257] the MEP has been applied in the study of electrostatic interaction. But it has been the group of Politzer who has used this scalar field extensively to gain in the understanding of general electrophilic substitution reactions and many other chemical applications.[258,259] Some works by Politzer, mainly dealing with benzenoid systems, have contributed toward establishing the MEP as a key entity to analyze the properties of the π-regions in molecules.[251,260]

A beautiful example of the relationship between the topology of the MEP and molecular reactivity is given by Klarner and Kahlert.[261] They studied molecular tweezers and clips containing naphthalene and benzene spacer units. The molecular tweezers and clips serve as receptors for electron-deficient neutral and cationic substrates. These findings can be explained with the electrostatic potential surface (EPS, Figure 21). The EPS is negative for pure hydrocarbons on the concave side of each molecule, whereas on the convex side it is less negative, corresponding to that of tetraalkyl-substituted arenes such as durene. When analogous calculations were performed for aromatic and aliphatic substrates, which form complexes with the molecular tweezers and clips, the complementary nature of their electrostatic potential surface to that inside the receptor cavities becomes evident. They suggest that the receptor−substrate interactions reported for the tweezers and clips are predominantly of electrostatic nature. But most fascinating is that they rationalized the results of the EPS calculations in terms of the topology of the MEP. If two π-electron systems are linearly connected but not conjugated and the distance between them is large enough, a positive test charge at a position close to the first π system (Figure 21, left side) interacts only with the first π system and not with the second one, so that the MEP in this case is not influenced by the introduction of the second π system. However, if the molecule is bent, as it is in the case of the tweezers and clips, the two π systems at the same distance as in the first case (Figure 21, right side) approach each other on the concave side and the potential becomes more negative by the introduction of the second π system. This is a general phenomenon of all nonconjugated π systems having concave−convex topography, which, for example, also explains the binding properties of cyclophane-type receptors.

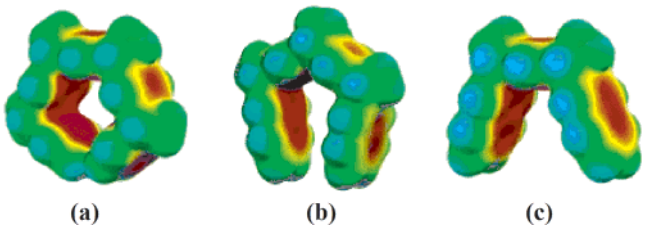

Figure 21. EPS of (a) tweezers and (b,c) two clips. The results of the AM1 calculations are depicted. The color code spans from −25 (red) to +25 kcal/mol (blue). Reprinted with permission from ref 261. Copyright 2003 American Chemical Society.

The group of Gadre devoted considerable effort to understand the topology of the electrostatic potential. Gadre and his collaborators showed that a detailed investigation of the topology of the MEP is capable of revealing subtle changes of the spatial electronic distribution due to changes in the molecular framework.[10,262,263] The MEP has different types of CPs that can be used to assign the molecular structure.[264] Leboeuf et al. have argued that lone pairs and π bonds, giving rise to electron rich regions "far" from the nuclei, will induce negative minima in the MEP. Gadre and other authors have illustrated that the minima of the MEP act as potential binding sites toward a positively charged species or the electron-deficient regions of a neutral molecule.[252,265,266]

Let us compare the MEP of benzene and cyclobutadiene. Benzene exhibits a perfect circular distribution of six −(3, +3) minima connected by the six −(3, +1) saddles all observed at a distance of 1.94 Å above the ring (Figure 22).[264,267,268] This reflects the attractive nature of the π system for electrophiles and that all C−C bonds are equivalent. In contrast, the minima above and below the C−C double bonds are not directly over the bonds in cyclobutadiene but are shifted toward the outside of the ring. Furthermore, two saddle points of −(3, +1) signature and not four (as would be needed for a "conjugation") connect them.[264]

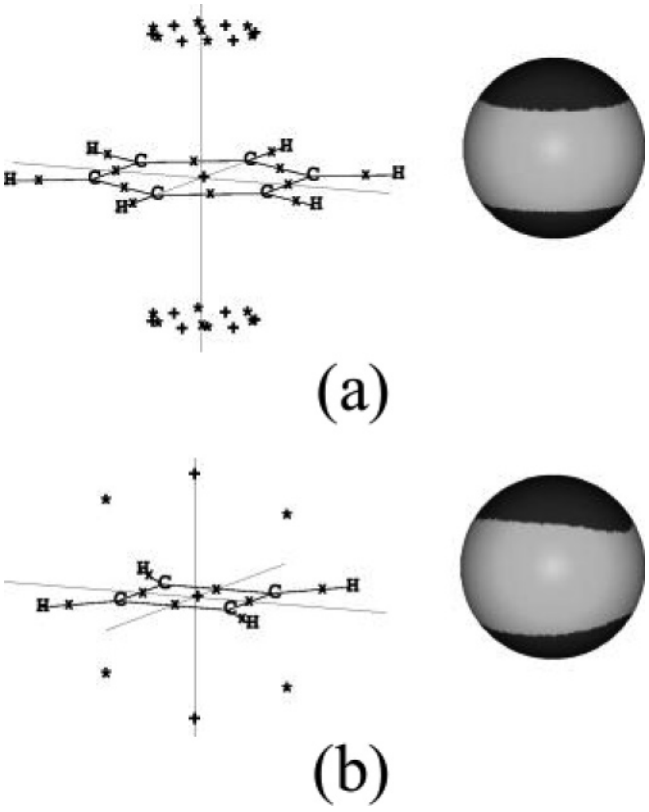

Figure 22. CP of the MEP for (a) benzene and (b) cyclobutadiene. The symbols × and + are the −(3, −1) and −(3, +1) CPs, respectively. Reprinted with permission from ref 264. Copyright 1999 American Institute of Physics.

In 1995, Gadre and Pundlik studied molecules containing benzene annulated to one or more of three- or four-membered rings.[269] They found that there is a "push−pull" effect of charge in systems with both types of rings and quantified this observation in terms of values of the MEP. Suresh and Gadre found that a MEP minimum over an aromatic nucleus provides a direct measure for the electronic perturbations due to a particular substituent.[270,271]

The sextet rule of Clar is an extension of aromaticity from monocyclic to fused polycyclic molecular systems.[272] Clar's sextet rule in benzenoid chemistry is equivalent to Lewis's octet rule in inorganic chemistry. Maximizing the number of Clar's sextets is analogous to maximizing the outer-shell electrons to a noble gas electronic configuration. Using the conjugated circuit theory, Randic has shown that total resonant sextet benzenoid hydrocarbon isomers have the highest resonance energy and states.[273] Suresh and Gadre explored the MEP topology of PAHs, attempting to define total aromaticity of the individual rings.[267] They show that the topological features of the MEP describe Clar's aromatic sextet theory very well and simplify the aromatic characterization of each ring of a PAH system. Each ring of all the annulated systems considered shows three or less (3, +3) CPs with different values. This suggests that only benzene has a perfect six π-delocalization, which is intimately connected with its high symmetry, whereas the hexagonal rings of all the annulated systems show varying degrees of π-localizations. Furthermore, the linear correlation of the MEP topography with local and global aromaticity indices provided by two independent theoretical results (those by Li and Jiang[274] and Zhou and Parr[275]) brings out a connection between aromaticity and the nature of π-electron distribution. Perhaps, the most encouraging aspect of the MEP topology is its ability to directly distinguish each ring of a PAH system simply by looking at the CP distribution.

Borazine is a representative aromatic inorganic molecule containing six π electrons delocalized over the six-membered ring. However, due to the large electronegativity difference between boron and nitrogen, one expects that the π-electron delocalization will be smaller in borazine than in benzene. Pukhan et al. presented a DFT-based study of the structure, stability, and reactivity of benzene, its linearly condensed compounds (naphthalene, anthracene, tetracene, and pentacene) and their BN analogues.[276] They noted that the prominent regions of negative electrostatic potential are on the nitrogen atoms and the hydrogens bound to boron. In borazine, the values of the MEP at their own CPs are not as negative as those in benzene. However, the hydrogen atoms attached to borons show a pronounced hydride character in terms of the MEP value. They suggested that the topology analysis of the MEP could be a powerful tool for studying a variety of chemical phenomena, in particular, the local π-electron concentrations explaining the aromatic character. The MEP topology patterns for acenes differ substantially from their respective BN analogues. BN-annulated systems show more localized π-electron features than the corresponding acene analogues. The average MEP function value at the CPs of individual rings indicates that the aromatic character in annulated acenes and their BN analogues is lowered thereby explaining "the aromatic dilution effect" as it is known in the literature.[272] However, the NICS values of acenes suggest that the middle rings of these systems are more aromatic (even than benzene) than the terminal ones. In this sense, the topology of the MEP offers a satisfactory explanation to various reactivity features of these annulated systems brought out by the earlier experimental and theoretical studies.

Finally, the topological analysis of the MEP has been applied to large carbon molecules. For instance, the analysis of C_{60} shows that all exo bonds to the five-membered rings have partial double-bond character with all molecular electrostatic potential minima located outside the molecular cage.[277] Peralta-Inga et al. investigated a series of two-dimensional sheets of hexagonal carbon rings, with hydrogens around the edges as models for graphene.[278] The potentials above the carbon rings are slightly negative, especially in the central portions of the systems.

7. Extension to Other Scalar and Vector Fields

Without going into too much detail, in this section, we browse through other molecular fields that have been used in the literature to describe electron delocalization.

7.1. Fukui Function

Recently, Lopez and Mendez studied the resonance forms of the imidazolium protonated cation using the Fukui function.[279] They claimed that it is possible to understand the resonance theory using this local reactivity index. However, no physical or mathematical justification supports this statement. Indeed, the Fukui function is an index of molecular reactivity,[6,280] and it has been studied systematically for a series of [*n*]-annulenes.[281] The expected reactivity of delocalized π orbitals in these aromatic molecules could be confirmed with this approach. However, it was not found to be useful to interpret Fukui functions or the related orbital hardness values as a measure of electron (de)localization.[281]

7.2. Magnetic Fields

Already in the early days of quantum chemistry, π-electron delocalization has been related to a ring current, which is induced if a magnetic field (that is, a vector field) is applied perpendicular to the ring plane. Such an induced π ring current was used, for the first time, by Pople to explain the abnormal ^{1}H NMR chemical shifts of benzene.[282] In Pople's model, the magnetic field induces a π ring current parallel to the molecular plane, which itself induces a magnetic field, which is enforcing the applied magnetic field at the positions of the benzene protons, lowering the shieldings. This model is under controversial scrutiny in the recent literature between the groups of Schleyer and Lazzeretti.[283−285] A projected π ring current in aromatic molecules has also been used to establish semiempirical methods for the determination of NMR chemical shifts.[286] The Pople model, and even some of its refinements, is nowadays used in text books to explain magnetic properties of aromatic molecules, and the magnetic criterion for aromaticity is today the most often applied one.[136,287] Because several review articles[126,127,287,288] deal with induced ring currents, we will not discuss this topic here in detail. We will, however, briefly review the topological analysis of the current density, which is the underlying quantity for an induced π ring current, and discuss its relation to electron delocalization.

The induced current density, $\mathbf{j}(\mathbf{r})$, is a three-component vector field. When discussed considering relativistic influences, which are often necessary if an external vector potential is present, the four-component relativistic current density has to be used instead.[289,290] While for the relativistic case no topological analysis has been performed yet, the nonrelativistic induced current density has been discussed a few times in the literature. The relevant mathematical background has been developed by Gomes in the early 1980s,[291−294] and detailed reviews, including mathematical and physical background, were given at beginning of the millennium.[136,287] Most importantly, the stagnation points, (3, +1) critical points where the current density is zero, and stagnation lines, (2, 0) critical "axis", are necessary for establishing a ring current effect, but also for other special positions of the current density.

Whether a region of current flow is diamagnetic or paramagnetic depends on the curl of the current density, $\nabla \times \mathbf{j}(\mathbf{r})$, at the (3, +1) critical point, relative to the atomic shell structure. The three-dimensional field $\nabla \times \mathbf{j}(\mathbf{r})$ is also called a *vorticity* field.[13,295] While plenty of current density maps of molecules have been produced in the past decade,[136,287] we are only aware of one detailed analysis of the current density applied to some example cases by Keith and Bader, published more than 10 years ago.[13,295] There might be several reasons for the unpopularity of this method: First, there is still the drawback of availability of methods producing magnetically induced current densities in popular quantum-chemistry packages. They have been restricted either to the in praxi inapplicable *common gauge* approach,[296] or to the continuous set of gauge transformations (CSGT),[297] or to the similar continuous transformation of the current density (CTOCD)[298] approaches. Only recently, the current density has been calculated using gauge-including atomic orbitals (GIAO),[299,300] as proposed by Juselius et al. in the gauge-including magnetic induced current (GIMIC) scheme,[301] after the pioneering work of Keith in 1996.[299] Second, in most applications the overall appearance the magnitude of the current density is discussed without stressing the CPs of this quantity. Up to today, unfortunately, discussing a vector field is still not rationalized on solid mathematical grounds by its topological analysis. In the only application of the topological analysis of the current density, Keith and Bader found that in benzene the basins of the current density *mimic* that of the Laplacian of the electron density. The topological analysis of vector fields might become more popular in the future because more molecular vector fields have been calculated recently. For example, the knowledge of the magnetic shielding function of a molecule gives direct access to the induced magnetic field.[119] In principle, the induced electric field can be accessed in an analogous way through the polarizability tensor, and such applications become important in the new field of nanoelectronics or in the design of nonlinear optical devices.

7.3. Molecular Fields Related to the Pair Density

In 1998, Gillespie et al. showed that a related distribution function, the conditional probability for same-spin electrons or Lennard-Jones function, LJF-($\mathbf{r}_2$,$\mathbf{r}_1$),

$$\mathrm{LJF}(\mathbf{r}_1,\mathbf{r}_2) = \rho^{\sigma}(\mathbf{r}_1) + h_{\sigma\sigma}(\mathbf{r}_1,\mathbf{r}_2) \qquad (42)$$

is successful in recovering the models associated with differing numbers of electron pairs.[302] The maxima in the LJF($\mathbf{r}_2$,$\mathbf{r}_1$) show where the density of the other electrons, relative to a fixed position of a same-spin reference electron, is most likely to be found, as illustrated in Figure 23. The function quantitatively measures the extent of exclusion of the density of one electron from that of another electron of the same spin. There is a remarkable similarity in the patterns of spatial pairing exhibited by LJF($\mathbf{r}_2$,$\mathbf{r}_1$) and of $L(\mathbf{r})$. On the other hand, the physical background of LJF-($\mathbf{r}_2$,$\mathbf{r}_1$) could be analyzed by studying both functions. The mechanism how the two-electron correlation,

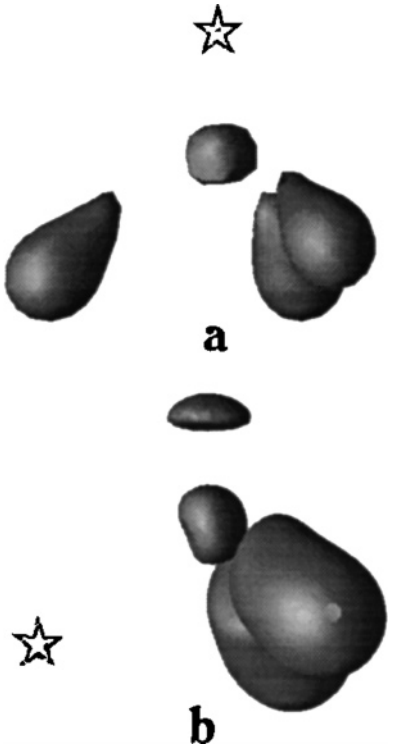

Figure 23. Envelope of Lennard-Jones function maps for PH_3. In panel a, the reference electron is at the position of the nonbonding maximum as indicated by a star, and the same-spin density is localized on the three protons, displayed with an envelope value = 0.15 au. In panel b, the reference electron is at the position of a proton, and the same-spin density is localized on the remaining two protons and in the nonbonding region, shown with an envelope value = 0.06 au. Same-spin density is localized within the phosphorus core in both cases. Reprinted with permission from ref 302. Copyright 1998 American Chemical Society.

contained in $LJF(\mathbf{r}_2,\mathbf{r}_1)$, is transmitted to the density, and hence to $L(\mathbf{r})$, was accounted for. One disadvantage is that $LJF(\mathbf{r}_2,\mathbf{r}_1)$ requires the pair density for its evaluation, while the $ELF(\mathbf{r})$, for example, requires only the one-electron density matrix. Yet the information regarding the pairing of electrons yielded by both functions is empirically determined by the topology of the Laplacian of the one-electron density.

Recently, Karafiloglou investigated the context of Coulomb and exchange correlations with special emphasis given to the Coulomb correlations and their physical meaning.[303] He stresses that the two-center interactions of antiparallel spin electrons can be "repulsive" or "attractive" (as a direct consequence of chemical bonding), but the former are less important than the latter for the chemical bonding because they are determined by the magnitude of one-center interactions. The globally attractive two-center interactions are balanced by the repulsive one-center interactions. The molecular orbital wave functions of *cis*-butadiene were chosen as examples to illustrate the relative role of Coulomb and exchange interactions in chemical bonding. The magnitudes of exchange interactions are significantly larger (2−4 times) than those of the Coulomb interactions, and the two-center Coulomb and exchange correlations have opposite signs. Even though the CI is very crucial for Coulomb interactions, the exchange interactions, in general, are less sensitive. The provided description for chemical bonding is consistent with those of usual chemical electron pair pictures.

The order of electron pairs with antiparallel (Coulomb) and parallel (Fermi) spins, existing in a molecule, is quantified and compared by Karafiloglou and Panos.[304] They argued that information entropies provide a measure of the (dis)order of Coulomb and Fermi pairs. For the π-bonding of butadiene, taken as a model system, the (dis)order of electron pairs was examined at HF and CI levels, and it turned out that chemical bonding imposes an increase both Coulomb and Fermi pairs. However, Fermi pairs have been found to be more ordered, that is, they involve more structure than the Coulomb ones. This holds remarkably well for all approximation levels.[304]

8. Conclusions

This article reviews the methodologies available to analyze molecular fields that are suitable descriptors of chemical bonding and electron delocalization. Special effort was given to summarize the mathematical and physical concepts necessary to perform the topological analysis of a molecular field. Several molecular fields relevant in chemistry to obtain information on the chemical bonding and, especially, on electron delocalization and electron localization, have been discussed in detail. These fields include the electron density, its Laplacian, the Fermi hole, the electrostatic potential, and a few other less common molecular fields.

The molecular fields discussed in this review are accessible either by the electron density or by the two-particle density matrix. While the descriptors based on the electron density are available for most methods of quantum chemistry and, quite importantly, for experimentally obtained electron densities, those descriptors requiring the two-particle density matrix are restricted to ab initio methods. In the current stage of development, they are not applicable within DFT, except if models of the two-particle density are used.

Most of the descriptors of molecular fields that have been proposed in the literature are included, even if today their use has been discarded, for example, Loge theory. However, since the most common reason for dropping a given approach or a theory was its mathematical or computational complexity and considering the enormous progress in theory, algorithms, computer technology, and, vital for this field, computer graphics, one can expect the renaissance of some approaches. This is the fundamental reason to include some "obsolete" descriptors of the chemical bond. The implementation of these analytical methodologies in popular quantum chemistry software will soon make these intensive studies a standard and routine computational task, contributing to our understanding of the electron localization and delocalization phenomena. For the sake of a coherent mathematical description we throughout applied localized basis functions to the reviewed methodology, because it simplifies mathematical expressions and allows a mathematical description familiar to most chemists. Consequently, the applications of well-known plane

wave methodology to the evaluation of some of the fields and descriptors reviewed were not considered.

In the not too distant past, the mathematically demanding apparatus needed for the topological analysis restricted its application to small molecules or larger ones having an extraordinarily high symmetry. As it is shown in the review, with the current machinery the analysis of complex organic and biological molecules is becoming feasible. The analysis of molecular fields of systems containing heavier nuclei is still a challenge, because the electron count is large and because relativistic effects start to be important. Moreover, even before considering the study of heavy atom containing systems, more work has to be done around the analysis of different molecular fields (scalar and vector) in transition metal complexes. Undoubtedly, this is one of the current challenges in the field.

The topological analysis of the electron density and related molecular fields is a bridge between theory and experiment. Since the electron density can be accessed experimentally as well as computed theoretically, its detailed topological analysis allows an interesting interplay between theory and experiment, allowing further improvements in experimental techniques and approaches in quantum chemistry in a very nice and healthy synergistic way.

We discussed deeply those molecular descriptors directly related to the electronic structure of unperturbed molecules, including the electron density, its Laplacian, the Fermi hole, and the electrostatic potential. The list is obviously incomplete without the electron localization function (ELF). This very important molecular scalar field is reviewed by Sola and Silvi[20] in this issue of *Chemical Reviews* and is therefore not considered here. Furthermore, we briefly discuss molecular fields defined as or related to response properties, in particular, the current density and the induced magnetic field. These vector fields have been reviewed in detail in two other recent reviews[136,287] and are in part subject of another article in this issue.[137]

Finally, the extensive survey of applications of molecular fields and their descriptors, discussed in this review and used in the literature to gain more chemical and physical insight on the problem of electron delocalization, shows that restricting the analysis to a single descriptor or molecular field may be contradictory or inconclusive. In contrast, the panoramic view gained by the application of different descriptors and different molecular fields is not only complementary but, in many instances, mandatory for a better and coherent understanding of the underlying mechanisms of electron localization and delocalization that contribute to the chemical binding in molecular systems, a topic that is certainly far from been closed.

9. Acronyms

VB	valence bond
MO	molecular orbital
HF	Hartree−Fock
ELF	electron localization function
CP	critical point
BCP	bond critical point
CPDED	critical point descriptor of electron density
PAH	polycyclic aromatic hydrocarbon
HOMA	harmonic oscillator model of aromaticity
NICS	nucleus-independent chemical shifts
PBA	1,3-propylenebis(oxamato)
RAHB	resonance-assisted hydrogen bond
QTMS	quantum topological molecular similarity
KS	Kohn−Sham
VSCC	valence-shell charge concentration
VSEPR	valence-shell electron pair repulsion
CC	charge concentration
CD	charge depletion
CI	configuration interaction
KS-DFT	Kohn−Sham density functional theory
MP2	second-order Møller−Plesset perturbation theory
MP4	fourth-order Møller−Plesset perturbation theory
CISD	single and double excitations, single reference configuration interaction method
QCISD	quadratic CI with single and double excitations
B3LYP	Becke 3, Lee, Yang, and Parr
ROHF	restricted open shell HF
UHF	unrestricted HF
IRC	intrinsic reaction path
ASE	aromatic stabilization energy
DI	delocalization index
PDI	para delocalization index
HOMO	highest occupied molecular orbital
LUMO	lowest unoccupied molecular orbital
MEP	molecular electrostatic potential
CSGT	continuous set of gauge transformations
CTOCD	continuous transformation of the current density
GIAO	gauge-including atomic orbitals
GIMIC	gauge-including magnetic induced current
LJF	Lennard-Jones function

10. Acknowledgments

The authors are grateful for financial support from the Deutsche Forschungsgemeinschaft (DFG). Invaluable technical help was provided by Viktoria Ivanovskaya and Catalina Ibarra. A.V. wishes to acknowledge the grants from Conacyt Projects G34037-E and G32710-E.

11. References

(1) Muller, P. *Pure Appl. Chem.* **1994**, *66*, 1077.
(2) Coulson, C. A. *Valence*; Clarendon Press: Oxford, U.K., 1952.
(3) Lloyd, D.; Marshall, D. R. In *Aromaticity, pseudo-aromaticity, anti-aromaticity; proceedings of an international symposium held in Jerusalem, 31 March-3 April, 1970*; Bergmann, E. D., Pullman, B., Eds.; Jerusalem symposia on quantum chemistry and biochemistry 3; Israeli Academy of Sciences: Jerusalem, 1971.
(4) Reed, A. E.; Curtiss, L. A.; Weinhold, F. *Chem. Rev.* **1988**, *88*, 899.
(5) McWeeny, R.; Sutcliffe, B. T. *Methods of Molecular Quantum Mechanics*; Academic Press: London, 1969.
(6) Parr, R. G.; Yang, W. *Density Functional Theory of Atoms and Molecules*; Oxford University Press: Oxford, England, 1989.
(7) Davidson, E. R. *Reduced Density Matrixes in Quantum Chemistry*; Academic Press: New York, 1976.
(8) Koritsanszky, T. S.; Coppens, P. *Chem. Rev.* **2001**, *101*, 1583.
(9) Hohenberg, P.; Kohn, W. *Phys. Rev. B* **1964**, *136*, 864.
(10) Pathak, R. K.; Gadre, S. R. *J. Chem. Phys.* **1990**, *93*, 1770.
(11) Savin, A.; Nesper, R.; Wengert, S.; Fassler, T. F. *Angew. Chem., Int. Ed. Engl.* **1997**, *36*, 1809.
(12) Bader, R. F. W.; Essen, H. *J. Chem. Phys.* **1984**, *80*, 1943.
(13) Keith, T. A.; Bader, R. F. W. *J. Chem. Phys.* **1993**, *99*, 3669.
(14) Bader, R. F. W.; Heard, G. L. *J. Chem. Phys.* **1999**, *111*, 8789.
(15) Bader, R. F. W. *Chem. Rev.* **1991**, *91*, 893.
(16) Bader, R. F. W. *Acc. Chem. Res.* **1985**, *18*, 9.
(17) Bader, R. F. W. *Atoms in Molecules: A Quantum Theory*; Clarendon Press: Oxford, U.K., 1990.

(18) Popelier, P. L. A. *Mol. Phys.* **1996**, *87*, 1169.
(19) Popelier, P. L. A. *Coord. Chem. Rev.* **2000**, *197*, 169.
(20) Poater, J. M.; Duran, M.; Sola, M.; Silvi, B. *Chem. Rev.* **2005**, *105*, 3911.
(21) Collard, K.; Hall, G. G. *Int. J. Quantum. Chem.* **1977**, *12*, 623.
(22) Bader, R. F. W. *J. Phys. Chem. A* **1998**, *102*, 7314.
(23) Haaland, A.; Shorokhov, D. J.; Tverdova, N. V. *Chem.—Eur. J.* **2004**, *10*, 4416.
(24) Bader, R. F. W.; Fang, D.-C. *J. Chem. Theory Comput.* **2005**, *1*, 403.
(25) Bachrach, S. M. In *Reviews in Computational Chemistry*; Lipkowitz, K. B., Boys, D. B., Eds.; VCH Publishers: New York, 1994.
(26) Kohn, W.; Sham, L. J. *Phys. Rev.* **1965**, *140*, A1133.
(27) Bader, R. F. W.; Popelier, P. L. A.; Keith, T. A. *Angew. Chem., Int. Ed. Engl.* **1994**, *33*, 620.
(28) Bader, R. F. W.; Nguyendang, T. T.; Tal, Y. *Rep. Prog. Phys.* **1981**, *44*, 893.
(29) Bader, R. F. W. *Acc. Chem. Res.* **1975**, *8*, 34.
(30) Cremer, D.; Kraka, E. *J. Am. Chem. Soc.* **1985**, *107*, 3800.
(31) Bader, R. F. W.; Slee, T. S.; Cremer, D.; Kraka, E. *J. Am. Chem. Soc.* **1983**, *105*, 5061.
(32) Howard, S. T.; Krygowski, T. M. *Can. J. Chem.* **1997**, *75*, 1174.
(33) Krygowski, T. M.; Cyranski, M. K. *Chem. Rev.* **2001**, *101*, 1385.
(34) Schleyer, P. v. R.; Maerker, C.; Dransfeld, A.; Jiao, H. J.; Hommes, N. J. R. V. *J. Am. Chem. Soc.* **1996**, *118*, 6317.
(35) Mo, O.; Yanez, M.; Eckertmaksic, M.; Maksic, Z. B. *J. Org. Chem.* **1995**, *60*, 1638.
(36) Eckert-Maksic, M.; Glasovac, Z.; Maksic, Z. B. *J. Organomet. Chem.* **1998**, *571*, 65.
(37) Antol, I.; Glasovac, Z.; Hare, M. C.; Eckert-Maksic, M.; Kass, S. R. *Int. J. Mass Spectrom.* **2003**, *222*, 11.
(38) Roversi, P.; Barzaghi, M.; Merati, F.; Destro, R. *Can. J. Chem.* **1996**, *74*, 1145.
(39) Ranganathan, A.; Kulkarni, G. U. *J. Phys. Chem. A* **2002**, *106*, 7813.
(40) Molina, J. M.; El-Bergmi, R.; Dobado, J. A.; Portal, D. *J. Org. Chem.* **2000**, *65*, 8574.
(41) Raos, G.; Famulari, A.; Meille, S. V.; Gallazzi, M. C.; Allegra, G. *J. Phys. Chem. A* **2004**, *108*, 691.
(42) Jeffrey, G. A., Piniella, J. F., Eds. *The Application of Charge Density Research to Chemistry and Drug Design*; NATO ASI Series B, Physics, Vol. 250; Plenum Press: New York, 1991.
(43) Fuhrmann, P.; Koritsanszky, T.; Luger, P. *Z. Kristallogr.* **1997**, *212*, 213.
(44) Bianchi, R.; Gervasio, G.; Viscardi, G. *Acta Crystallogr. B* **1998**, *54*, 66.
(45) Yang, H. W.; Craven, B. M. *Acta Crystallogr. B* **1998**, *54*, 912.
(46) Gatti, C.; Frigerio, G.; Benincori, T.; Brenna, E.; Sannicolo, F.; Zotti, G.; Zecchin, S.; Schiavon, G. *Chem. Mater.* **2000**, *12*, 1490.
(47) Nyulaszi, L. *Inorg. Chem.* **1996**, *35*, 4690.
(48) Pizzonero, M.; Keller, L.; Dumas, F.; Ourevitch, M.; Morgant, G.; Bire, A. S. D.; Bogdanovic, G.; Ghermani, N. E.; d'Angelo, J. *J. Org. Chem.* **2004**, *69*, 4336.
(49) Pillet, S.; Souhassou, M.; Pontillon, Y.; Caneschi, A.; Gatteschi, D.; Lecomte, C. *New J. Chem.* **2001**, *25*, 131.
(50) Claiser, N.; Souhassou, M.; Lecomte, C.; Pontillon, Y.; Romero, F.; Ziessel, R. *J. Phys. Chem. B* **2002**, *106*, 12896.
(51) Pillet, S.; Souhassou, M.; Mathoniere, C.; Lecomte, C. *J. Am. Chem. Soc.* **2004**, *126*, 1219.
(52) Pillet, S.; Souhassou, M.; Lecomte, C. *Acta Crystallogr. A* **2004**, *60*, 455.
(53) Ziessel, R.; Stroh, C.; Heise, H.; Kohler, F. H.; Turek, P.; Claiser, N.; Souhassou, M.; Lecomte, C. *J. Am. Chem. Soc.* **2004**, *126*, 12604.
(54) Olah, G. A. *Hypercarbon Chemistry*; J. Wiley: New York, 1987.
(55) Okulik, N.; Peruchena, N.; Esteves, P. M.; Mota, C.; Jubert, A. H. *J. Phys. Chem. A* **2000**, *104*, 7586.
(56) Okulik, N. B.; Sosa, L. G.; Esteves, P. M.; Mota, C. J. A.; Jubert, A. H.; Peruchena, N. M. *J. Phys. Chem. A* **2002**, *106*, 1584.
(57) Lobayan, R. M.; Sosa, G. L.; Jubert, A. H.; Peruchena, N. M. *J. Phys. Chem. A* **2004**, *108*, 4347.
(58) Okulik, N.; Peruchena, N. M.; Esteves, P. M.; Mota, C. J. A.; Jubert, A. *J. Phys. Chem. A* **1999**, *103*, 8491.
(59) del Rio, E.; Menendez, M. I.; Lopez, R.; Sordo, T. L. *J. Phys. Chem. A* **2000**, *104*, 5568.
(60) Gilli, G.; Bellucci, F.; Ferretti, V.; Bertolasi, V. *J. Am. Chem. Soc.* **1989**, *111*, 1023.
(61) Gatti, C.; Saunders, V. R.; Roetti, C. *J. Chem. Phys.* **1994**, *101*, 10686.
(62) Grabowski, S. J.; Dubis, A. T.; Martynowski, D.; Glowka, M.; Palusiak, M.; Leszczynski, J. *J. Phys. Chem. A* **2004**, *108*, 5815.
(63) Malecka, M.; Grabowski, S. J.; Budzisz, E. *Chem. Phys.* **2004**, *297*, 235.
(64) Grabowski, S. J. *J. Mol. Struct.* **2001**, *562*, 137.
(65) Grabowski, S. J. *J. Phys. Org. Chem.* **2004**, *17*, 18.
(66) Rybarczyk-Pirek, A. J.; Grabowski, S. J.; Nawrot-Modranka, J. *J. Phys. Chem. A* **2003**, *107* (43), 9232.
(67) Wojtulewski, S.; Grabowski, S. J. *J. Mol. Struct. (THEOCHEM)* **2003**, *621*, 285.
(68) Grabowski, S. J. *Monatsh. Chem.* **2002**, *133*, 1373.
(69) Grabowski, S. J. *J. Phys. Org. Chem.* **2003**, *16*, 797.
(70) Alkorta, I.; Elguero, J. *J. Org. Chem.* **2002**, *67*, 1515.
(71) Madsen, G. K. H.; Iversen, B. B.; Larsen, F. K.; Kapon, M.; Reisner, G. M.; Herbstein, F. H. *J. Am. Chem. Soc.* **1998**, *120*, 10040.
(72) Schiott, B.; Iversen, B. B.; Madsen, G. K. H.; Bruice, T. C. *J. Am. Chem. Soc.* **1998**, *120*, 12117.
(73) Platts, J. A.; Howard, S. T.; Wozniak, K. *J. Org. Chem.* **1994**, *59*, 4647.
(74) Mallinson, P. R.; Wozniak, K.; Wilson, C. C.; McCormack, K. L.; Yufit, D. S. *J. Am. Chem. Soc.* **1999**, *121*, 4640.
(75) Merino, G., Study of the Chemical Bond via Topological Analysis of Molecular Scalar Fields. Ph.D. Thesis, Cinvestav, Mexico, D. F., Mexico, 2003.
(76) Merino, G.; Bakhmutov, V. I.; Vela, A. *J. Phys. Chem. A* **2002**, *106*, 8491.
(77) Guizado-Rodriguez, M.; Ariza-Castolo, A.; Merino, G.; Vela, A.; Noth, H.; Bakhmutov, V. I.; Contreras, R. *J. Am. Chem. Soc.* **2001**, *123*, 9144.
(78) Merino, G.; Mendez-Rojas, M. A.; Vela, A. *J. Am. Chem. Soc.* **2003**, *125*, 6026.
(79) Vela, A.; Merino, G. In *Reviews in Modern Quantum Chemistry: A Celebration of the Contributions of Robert Parr*; Sen, K. D., Ed.; World Scientific: Singapore, 2002.
(80) Merino, G.; Mendez-Rojas, M. A.; Beltran, H. I.; Corminboeuf, C.; Heine, T.; Vela, A. *J. Am. Chem. Soc.* **2004**, *126*, 16160.
(81) Dewar, M. J. S.; McKee, M. L. *Pure Appl. Chem.* **1980**, *52*, 1431.
(82) Wiberg, K. B.; Bader, R. F. W.; Lau, C. D. H. *J. Am. Chem. Soc.* **1987**, *109*, 985.
(83) Cremer, D.; Kraka, E.; Slee, T. S.; Bader, R. F. W.; Lau, C. D. H.; Nguyendang, T. T.; Macdougall, P. J. *J. Am. Chem. Soc.* **1983**, *105*, 5069.
(84) Cremer, D.; Schmidt, T.; Bock, C. W. *J. Org. Chem.* **1985**, *50*, 2684.
(85) Barzaghi, M.; Gatti, C. *J. Chim. Phys. Chim. Biol.* **1987**, *84*, 783.
(86) Gatti, C.; Barzaghi, M.; Simonetta, M. *J. Am. Chem. Soc.* **1985**, *107*, 878.
(87) Cremer, D.; Gauss, J. *J. Am. Chem. Soc.* **1986**, *108*, 7467.
(88) Cremer, D.; Kraka, E. *J. Am. Chem. Soc.* **1985**, *107*, 3811.
(89) Alcami, M.; Mo, O.; Yanez, M. *J. Comput. Chem.* **1998**, *19*, 1072.
(90) Koritsanszky, T.; Buschmann, J.; Luger, P. *J. Phys. Chem.* **1996**, *100*, 10547.
(91) Bader, R. F. W.; Legare, D. A. *Can. J. Chem.* **1992**, *70*, 657.
(92) Lyssenko, K. A.; Antipin, M. Y.; Lebedev, V. N. *Inorg. Chem.* **1998**, *37*, 5834.
(93) Bader, R. F. W.; Matta, C. F. *Inorg. Chem.* **2001**, *40*, 5603.
(94) Cortes-Guzman, F.; Bader, R. F. W. *Coord. Chem. Rev.* **2005**, *249*, 633.
(95) Bachrach, S. M. *J. Phys. Chem.* **1989**, *93*, 7780.
(96) Bachrach, S. M. *J. Org. Chem.* **1991**, *56*, 2205.
(97) Bachrach, S. M.; Salzner, U. *J. Mol. Struct. (THEOCHEM)* **1995**, *337*, 201.
(98) Moore, L.; Lubinski, R.; Baschky, M. C.; Dahlke, G. D.; Hare, M.; Arrowood, T.; Glasovac, Z.; EckertMaksic, M.; Kass, S. R. *J. Org. Chem.* **1997**, *62*, 7390.
(99) de Meijere, A.; Kozhushkov, S. I. *Chem. Rev.* **2000**, *100*, 93.
(100) Boese, R.; Miebach, T.; Demeijere, A. *J. Am. Chem. Soc.* **1991**, *113*, 1743.
(101) Yufit, D. S.; Mallinson, P. R.; Muir, K. W.; Kozhushkov, S. I.; DeMeijere, A. *Acta Crystallogr. B* **1996**, *52*, 668.
(102) Minkin, V. I.; Glukhovtsev, M. N.; Simkin, B. ë. *Aromaticity and antiaromaticity: electronic and structural aspects*; J. Wiley & Sons: New York, 1994.
(103) Sauers, R. R. *Tetrahedron* **1998**, *54*, 337.
(104) Moran, D.; Manoharan, M.; Heine, T.; Schleyer, P. v. R. *Org. Lett.* **2003**, *5*, 23.
(105) Liang, C. X.; Allen, L. C. *J. Am. Chem. Soc.* **1991**, *113*, 1878.
(106) Tafipolsky, M.; Scherer, W.; Ofele, K.; Artus, G.; Pedersen, B.; Herrmann, W. A.; McGrady, G. S. *J. Am. Chem. Soc.* **2002**, *124*, 5865.
(107) Scherer, W.; Sirsch, P.; Shorokhov, D.; McGrady, G. S.; Mason, S. A.; Gardiner, M. G. *Chem.—Eur. J.* **2002**, *8*, 2324.
(108) Scherer, W.; Sirsch, P.; Shorokhov, D.; Tafipolsky, M.; McGrady, G. S.; Gullo, E. *Chem.—Eur. J.* **2003**, *9*, 6057.
(109) Scherer, W.; McGrady, G. S. *Angew. Chem., Int. Ed.* **2004**, *43*, 1782.
(110) Popelier, P. L. A. *J. Phys. Chem. A* **1999**, *103*, 2883.
(111) O'Brien, S. E.; Popelier, P. L. A. *Can. J. Chem.* **1999**, *77*, 28.
(112) O'Brien, S. E.; Popelier, P. L. A. *J. Chem. Inf. Comput. Sci.* **2001**, *41*, 764.
(113) O'Brien, S. E.; Popelier, P. L. A. *J. Chem. Soc., Perkin Trans. 2* **2002**, 478.
(114) Platts, J. A. *Phys. Chem. Chem. Phys.* **2000**, *2*, 3115.
(115) Platts, J. A. *Phys. Chem. Chem. Phys.* **2000**, *2*, 973.
(116) Matta, C. F. *J. Comput. Chem.* **2003**, *24*, 453.

(117) Matta, C. F.; Hernandez-Trujillo, J.; Tang, T. H.; Bader, R. F. W. *Chem.—Eur. J.* **2003**, *9*, 1940.
(118) Popelier, P. L. A.; Chaudry, U. A.; Smith, P. J. *J. Chem. Soc., Perkin Trans. 2* **2002**, 1231.
(119) Merino, G.; Heine, T.; Seifert, G. *Chem.—Eur. J.* **2004**, *10*, 4367.
(120) Schleyer, P. v. R.; Manoharan, M.; Wang, Z. X.; Kiran, B.; Jiao, H. J.; Puchta, R.; Hommes, N. J. R. V. *Org. Lett.* **2001**, *3*, 2465.
(121) Kaupp, M.; Bühl, M.; Malkin, V. G. *Calculation of NMR and EPR parameters: Theory and Applications*; Wiley-VCH: Weinheim, Germany, 2004.
(122) Morao, I.; Lecea, B.; Cossio, F. P. *J. Org. Chem.* **1997**, *62*, 7033.
(123) Subramanian, G.; Schleyer, P. v. R.; Dransfeld, A. *Organometallics* **1998**, *17*, 1634.
(124) Cossio, F. P.; Morao, I.; Jiao, H. J.; Schleyer, P. v. R. *J. Am. Chem. Soc.* **1999**, *121*, 6737.
(125) Alkorta, I.; Elguero, J. *New J. Chem.* **1999**, *23*, 951.
(126) Nguyen, L. T.; De Proft, F.; Nguyen, M. T.; Geerlings, P. *J. Chem. Soc., Perkin Trans. 2* **2001**, 898.
(127) de Lera, A. R.; Alvarez, R.; Lecea, B.; Torrado, A.; Cossio, F. P. *Angew. Chem., Int. Ed.* **2001**, *40*, 557.
(128) Morao, I.; Hillier, I. H. *Tetrahedron Lett.* **2001**, *42*, 4429.
(129) Bachrach, S. M. *J. Organomet. Chem.* **2002**, *643*−*644*, 39.
(130) Rodriguez-Otero, J.; Martinez-Nunez, E.; Pena-Gallego, A.; Vazquez, S. A. *J. Org. Chem.* **2002**, *67*, 6347.
(131) Quinonero, D.; Prohens, R.; Garau, C.; Frontera, A.; Ballester, P.; Costa, A.; Deya, P. M. *Chem. Phys. Lett.* **2002**, *351*, 115.
(132) Rodriguez-Otero, J.; Cabaleiro-Lago, E. M. *Chem.—Eur. J.* **2003**, *9*, 1837.
(133) Alkorta, I.; Elguero, J.; Eckert-Maksic, M.; Maksic, Z. B. *Tetrahedron* **2004**, *60*, 2259.
(134) Winkler, M.; Cakir, B.; Sander, W. *J. Am. Chem. Soc.* **2004**, *126*, 6135.
(135) Rodriguez-Otero, J.; Cabaleiro-Lago, E. M.; Hermida-Ramon, J. M.; Pena-Gallego, A. *J. Org. Chem.* **2003**, *68*, 8823.
(136) Gomes, J. A. N. F.; Mallion, R. B. *Chem. Rev.* **2001**, *101*, 1349.
(137) Heine, T.; Corminboeuf, C.; Seifert, G. *Chem. Rev.* **2005**, *105*, 3889.
(138) Pauling, L. *The Nature of the Chemical Bond and the Structure of Molecules and Crystals; An Introduction to Modern Structural Chemistry*; Cornell Univerity Press: Ithaca, NY, 1960.
(139) Ponec, R.; Yuzhakov, G.; Cooper, D. L. *J. Phys. Chem. A* **2003**, *107*, 2100.
(140) Cioslowski, J.; Mixon, S. T. *J. Am. Chem. Soc.* **1991**, *113*, 4142.
(141) Wiberg, K. B. *J. Org. Chem.* **1997**, *62*, 5720.
(142) Fulton, R. L. *J. Phys. Chem.* **1993**, *97*, 7516.
(143) Fulton, R. L.; Mixon, S. T. *J. Phys. Chem.* **1993**, *97*, 7530.
(144) Mitrasinovic, P. M. *J. Comput. Chem.* **2001**, *22*, 1387.
(145) Mitrasinovic, P. M. *J. Phys. Chem. A* **2002**, *106*, 7026.
(146) Mitrasinovic, P. M. *Chem. Phys.* **2003**, *286*, 1.
(147) Angyan, J. G.; Loos, M.; Mayer, I. *J. Phys. Chem.* **1994**, *98*, 5244.
(148) Kar, T.; Angyan, J. G.; Sannigrahi, A. B. *J. Phys. Chem. A* **2000**, *104*, 9953.
(149) Howard, S. T.; Lamarche, O. *J. Phys. Org. Chem.* **2003**, *16*, 133.
(150) Jules, J. L.; Lombardi, J. R. *J. Mol. Struct. (THEOCHEM)* **2003**, *664*, 255.
(151) Guggenheimer, K. M. *Proc. Phys. Soc.* **1946**, *63*, 456.
(152) Chesnut, D. B. *Chem. Phys.* **2003**, *291*, 141.
(153) Maxwell, J. C. *A Treatise on Electricity and Magnetism*, unabridged 3rd ed.; Dover Publcations: New York, 1954.
(154) Bader, R. F. W.; Macdougall, P. J.; Lau, C. D. H. *J. Am. Chem. Soc.* **1984**, *106*, 1594.
(155) Bader, R. F. W.; Beddall, P. M. *J. Chem. Phys.* **1972**, *56*, 3320.
(156) Malcolm, N. O. J.; Popelier, P. L. A. *J. Phys. Chem. A* **2001**, *105*, 7638.
(157) Malcolm, N. O. J.; Popelier, P. L. A. *Faraday Discuss.* **2003**, *124*, 353.
(158) Gillespie, R. J.; Hargittai, I. *The VSEPR Model of Molecular Geometry*; Allyn and Bacon: Boston, MA, 1991.
(159) Gillespie, R. J.; Popelier, P. L. A. *Chemical Bonding and Molecular Geometry: from Lewis to Electron Densities*; Oxford University Press: New York, 2001.
(160) Bader, R. F. W.; Stephens, M. E. *J. Am. Chem. Soc.* **1975**, *97*, 7391.
(161) Bader, R. F. W.; Gillespie, R. J.; Macdougall, P. J. *J. Am. Chem. Soc.* **1988**, *110*, 7329.
(162) Bader, R. F. W.; Johnson, S.; Tang, T. H.; Popelier, P. L. A. *J. Phys. Chem.* **1996**, *100*, 15398.
(163) Gobbi, A.; Frenking, G. *J. Am. Chem. Soc.* **1994**, *116*, 9287.
(164) Gobbi, A.; Frenking, G. *J. Am. Chem. Soc.* **1994**, *116*, 9275.
(165) Cioslowski, J.; Mixon, S. T.; Fleischmann, E. D. *J. Am. Chem. Soc.* **1991**, *113*, 4751.
(166) Gobbi, A.; Frenking, G. *J. Am. Chem. Soc.* **1993**, *115*, 2362.
(167) Marchand, C. M.; Pidun, U.; Frenking, G.; Grutzmacher, H. *J. Am. Chem. Soc.* **1997**, *119*, 11078.
(168) Boehme, C.; Frenking, G. *J. Am. Chem. Soc.* **1996**, *118*, 2039.
(169) Heinemann, C.; Muller, T.; Apeloig, Y.; Schwarz, H. *J. Am. Chem. Soc.* **1996**, *118*, 2023.
(170) Munoz-Caro, C.; Nino, A.; Senent, M. L.; Leal, J. M.; Ibeas, S. *J. Org. Chem.* **2000**, *65*, 405.
(171) Garcia-Viloca, M.; Gonzalez-Lafont, A.; Lluch, J. M. *J. Am. Chem. Soc.* **1997**, *119*, 1081.
(172) Mo, O.; Yanez, M.; Esseffar, M.; Herreros, M.; Notario, R.; Abboud, J. L. M. *J. Org. Chem.* **1997**, *62*, 3200.
(173) Daudel, R.; Brion, H.; Odiot, S. *J. Chem. Phys.* **1955**, *23*, 2080.
(174) Aslangui, R.; Constanciel, R.; Daudel, R.; Kottis, P. *Adv. Quantum Chem.* **1972**, *6*, 93.
(175) Daudel, R.; Bader, R. F. W.; Stephens, M. E.; Borrett, D. S. *Can. J. Chem.* **1974**, *52*, 1310.
(176) Bader, R. F. W.; Stephens, M. E. *Chem. Phys. Lett.* **1974**, *26*, 445.
(177) Levy, M. *J. Am. Chem. Soc.* **1976**, *98*, 6849.
(178) Lennard-Jones, J. *Proc. R. Soc. London, Ser. A* **1949**, *198*, 14.
(179) Lennard-Jones, J. *J. Chem. Phys.* **1952**, *20*, 1024.
(180) Lennard-Jones, J. *Adv. Sci. London* **1954**, *11*.
(181) McWeeny, R. *Rev. Mod. Phys.* **1960**, *32*, 335.
(182) McWeeny, R. *Methods of Molecular Quantum Mechanics*, 2nd ed.; Academic Press: London, San Diego, CA, 1989.
(183) Wigner, E. P.; Seitz, F. *Phys. Rev.* **1934**, *46*, 509.
(184) Salem, L. *The molecular orbital theory of conjugated systems*; W. A. Benjamin: New York, 1966.
(185) Matta, C. F.; Hernandez-Trujillo, J.; Bader, R. F. W. *J. Phys. Chem. A* **2002**, *106*, 7369.
(186) Fradera, X.; Austen, M. A.; Bader, R. F. W. *J. Phys. Chem. A* **1999**, *103*, 304.
(187) Molina, J. M.; Dobado, J. A.; Heard, G. L.; Bader, R. F. W.; Sundberg, M. R. *Theor. Chem. Acc.* **2001**, *105*, 365.
(188) Ponec, R.; Mayer, I. *J. Phys. Chem. A* **1997**, *101*, 1738.
(189) Bochicchio, R.; Lain, L.; Torre, A.; Ponec, R. *J. Math. Chem.* **2000**, *28*, 83.
(190) Bochicchio, R.; Ponec, R.; Torre, A.; Lain, L. *Theor. Chem. Acc.* **2001**, *105*, 292.
(191) Bent, H. A. *Inorg. Chem.* **1963**, *2*, 747.
(192) Laidig, K. E.; Cameron, L. M. *J. Am. Chem. Soc.* **1996**, *118*, 1737.
(193) Bader, R. F. W.; Streitwieser, A.; Neuhaus, A.; Laidig, K. E.; Speers, P. *J. Am. Chem. Soc.* **1996**, *118*, 4959.
(194) Wang, C. C.; Wang, Y.; Liu, H. J.; Lin, K. J.; Chou, L. K.; Chan, K. S. *J. Phys. Chem. A* **1997**, *101*, 8887.
(195) Hwang, T. S.; Wang, Y. *J. Phys. Chem. A* **1998**, *102*, 3726.
(196) Lee, C. R.; Wang, C. C.; Chen, K. C.; Lee, G. H.; Wang, Y. *J. Phys. Chem. A* **1999**, *103*, 156.
(197) Wang, C. C.; Tang, T. H.; Wang, Y. *J. Phys. Chem. A* **2000**, *104*, 9566.
(198) Lee, J. J.; Lee, G. H.; Wang, Y. *Chem.—Eur. J.* **2002**, *8*, 1821.
(199) Lee, C. R.; Tan, L. Y.; Wang, Y. *J. Phys. Chem. Solids* **2001**, *62*, 1613.
(200) Wang, C. C.; Tang, T. H.; Wu, L. C.; Wang, Y. *Acta Crystallogr. A* **2004**, *60*, 488.
(201) Ponec, R. *J. Math. Chem.* **1997**, *21*, 323.
(202) Ponec, R. *J. Math. Chem.* **1998**, *23*, 85.
(203) Ponec, R.; Duben, A. J. *J. Comput. Chem.* **1999**, *20*, 760.
(204) Girones, X.; Carbo-Dorca, R.; Ponec, R. *J. Chem. Inf. Comput. Sci.* **2003**, *43*, 2033.
(205) Ponec, R.; Yuzhakov, G.; Girones, X.; Frenking, G. *Organometallics* **2004**, *23*, 1790.
(206) Bochicchio, R.; Ponec, R.; Lain, L.; Torre, A. *J. Phys. Chem. A* **2000**, *104*, 9130.
(207) Ponec, R.; Roithova, J. *Theor. Chem. Acc.* **2001**, *105*, 383.
(208) Ponec, R.; Roithova, J.; Girones, X.; Jug, K. *J. Mol. Struct. (THEOCHEM)* **2001**, *545*, 255.
(209) Ponec, R.; Girones, X. *J. Phys. Chem. A* **2002**, *106*, 9506.
(210) Ponec, R.; Roithova, J.; Girones, X.; Lain, L.; Torre, A.; Bochicchio, R. *J. Phys. Chem. A* **2002**, *106*, 1019.
(211) Ponec, R.; Yuzhakov, G.; Carbo-Dorca, R. *J. Comput. Chem.* **2003**, *24*, 1829.
(212) Poater, J.; Sola, M.; Duran, M.; Fradera, X. *Theor. Chem. Acc.* **2002**, *107*, 362.
(213) Wang, Y. G.; Werstiuk, N. H. *J. Comput. Chem.* **2003**, *24*, 379.
(214) Wang, Y. G.; Matta, C.; Werstiuk, N. H. *J. Comput. Chem.* **2003**, *24*, 1720.
(215) Poater, J.; Sola, M.; Duran, M.; Fradera, X. *J. Phys. Chem. A* **2001**, *105*, 2052.
(216) Fradera, X.; Poater, J.; Simon, S.; Duran, M.; Sola, M. *Theor. Chem. Acc.* **2002**, *108*, 214.
(217) Fradera, X.; Sola, M. *J. Comput. Chem.* **2002**, *23*, 1347.
(218) Bader, R. F. W.; Bayles, D. *J. Phys. Chem. A* **2000**, *104*, 5579.
(219) Poater, J.; Sola, M.; Duran, M.; Fradera, X. *J. Phys. Chem. A* **2001**, *105*, 6249.
(220) Gonzalez-Moa, M. J.; Mosquera, R. A. *J. Phys. Chem. A* **2003**, *107*, 5361.
(221) Mandado, M.; Mosquera, R. A.; Grana, A. M. *Chem. Phys. Lett.* **2004**, *386*, 454.
(222) Perez-Juste, I.; Graña, A. M.; Carballeira, L.; Mosquera, R. A. *J. Chem. Phys.* **2004**, *121*, 10447.
(223) Poater, J.; Fradera, X.; Sola, M.; Duran, M.; Simon, S. *Chem. Phys. Lett.* **2003**, *369*, 248.
(224) Daza, M. C.; Dobado, J. A.; Molina, J. M.; Villaveces, J. L. *Phys. Chem. Chem. Phys.* **2000**, *2*, 4089.
(225) Chesnut, D. B. *J. Phys. Chem. A* **2003**, *107*, 4307.

(226) Chesnut, D. B.; Quin, L. D. *J. Comput. Chem.* **2004**, *25*, 734.
(227) Chesnut, D. B.; Quin, L. D. *Heteroatom Chem.* **2004**, *15*, 216.
(228) Chesnut, D. B.; Quin, L. D.; Seaton, P. J. *Magn. Reson. Chem.* **2004**, *42*, S20.
(229) El-Bergmi, R.; Dobado, J. A.; Portal, D.; Molina, J. M. *J. Comput. Chem.* **2000**, *21*, 322.
(230) Chesnut, D. B. *Heteroatom Chem.* **2002**, *13*, 53.
(231) Chesnut, D. B. *Heteroatom Chem.* **2003**, *14*, 175.
(232) Dobado, J. A.; Martinez-Garcia, H.; Molina, J. M.; Sundberg, M. R. *J. Am. Chem. Soc.* **2000**, *122*, 1144.
(233) Sanchez-Gonzalez, A.; Martinez-Garcia, H.; Melchor, S.; Dobado, J. A. *J. Phys. Chem. A* **2004**, *42*, 9188.
(234) Luana, V.; Pendas, A. M.; Costales, A.; Carriedo, G. A.; Garcia-Alonso, F. J. *J. Phys. Chem. A* **2001**, *105*, 5280.
(235) Dobado, J. A.; Molina, J. M.; Uggla, R.; Sundberg, M. R. *Inorg. Chem.* **2000**, *39*, 2831.
(236) Poater, J.; Cases, M.; Fradera, X.; Duran, M.; Sola, M. *Chem. Phys.* **2003**, *294*, 129.
(237) Macchi, P.; Garlaschelli, L.; Sironi, A. *J. Am. Chem. Soc.* **2002**, *124*, 14173.
(238) Tomaszewski, R.; Hyla-Kryspin, I.; Mayne, C. L.; Arif, A. M.; Gleiter, R.; Ernst, R. D. *J. Am. Chem. Soc.* **1998**, *120*, 2959.
(239) Matta, C. F.; Hernandez-Trujillo, J. *J. Phys. Chem. A* **2003**, *107*, 7496.
(240) Poater, J.; Duran, M.; Sola, M. *Int. J. Quantum Chem.* **2004**, *98*, 361.
(241) Chesnut, D. B.; Bartolotti, L. J. *Chem. Phys.* **2000**, *257*, 175.
(242) Hernandez-Trujillo, J.; Garcia-Cruz, I.; Martinez-Magadan, J. M. *Chem. Phys.* **2005**, *308*, 181.
(243) Matta, C. F.; Cow, C. N.; Harrison, P. H. M. *J. Mol. Struct.* **2003**, *660*, 81.
(244) Werstiuk, N. H.; Wang, Y. G. *J. Phys. Chem. A* **2001**, *105*, 11515.
(245) Werstiuk, N. H.; Wang, Y. G. *J. Phys. Chem. A* **2003**, *107*, 9434.
(246) Poater, J.; Fradera, X.; Duran, M.; Sola, M. *Chem.—Eur. J.* **2003**, *9*, 400.
(247) Poater, J.; Fradera, X.; Duran, M.; Sola, M. *Chem.—Eur. J.* **2003**, *9*, 1113.
(248) Krygowski, T. M.; Ejsmont, K.; Stepien, B. T.; Cyranski, M. K.; Poater, J.; Sola, M. *J. Org. Chem.* **2004**, *69*, 6634.
(249) Poater, J.; Garcia-Cruz, I.; Illas, F.; Sola, M. *Phys. Chem. Chem. Phys.* **2004**, *6*, 314.
(250) Poater, J.; Sola, M.; Viglione, R. G.; Zanasi, R. *J. Org. Chem.* **2004**, *69*, 7537.
(251) Politzer, P.; Truhlar, D. G. *Chemical Applications of Atomic and Molecular Electrostatic Potentials*; Plenum Press: New York, 1981.
(252) Murray, J. S.; Sen, K. D. *Molecular Electrostatic Potentials: Concepts and Applications*; Elsevier: Amsterdam, New York, 1996.
(253) Naray-Szabo, G.; Ferenczy, G. G. *Chem. Rev.* **1995**, *95*, 829.
(254) Pullman, A.; Pullman, B. *Q. Rev. Biophys.* **1981**, *14*, 289.
(255) Tomasi, J.; Persico, M. *Chem. Rev.* **1994**, *94*, 2027.
(256) Scrocco, E.; Tomasi, J. *Fortschr. Chem. Forsch.* **1973**, *42*, 95.
(257) Scrocco, E.; Tomasi, J. *Adv. Quantum Chem.* **1978**, *11*, 115.
(258) Politzer, P.; Abrahmsen, L.; Sjoberg, P. *J. Am. Chem. Soc.* **1984**, *106*, 855.
(259) Sjoberg, P.; Politzer, P. *J. Phys. Chem.* **1990**, *94*, 3959.
(260) Murray, J. S.; Abu-Awwad, F.; Politzer, P. *J. Mol. Struct. (THEOCHEM)* **2000**, *501*, 241.
(261) Klarner, F. G.; Kahlert, B. *Acc. Chem. Res.* **2003**, *36*, 919.
(262) Gadre, S. R.; Kulkarni, S. A.; Shrivastava, I. H. *J. Chem. Phys.* **1992**, *96*, 5253.
(263) Shirsat, R. N.; Bapat, S. V.; Gadre, S. R. *Chem. Phys. Lett.* **1992**, *200*, 373.
(264) Leboeuf, M.; Koster, A. M.; Jug, K.; Salahub, D. R. *J. Chem. Phys.* **1999**, *111*, 4893.
(265) Gadre, S. R.; Pingale, S. S. *Chem. Commun.* **1996**, 595.
(266) Mehta, G.; Ravikrishna, C.; Gadre, S. R.; Suresh, C. H.; Kalyanaraman, P.; Chandrasekhar, J. *Chem. Commun.* **1998**, 975.
(267) Suresh, C. H.; Gadre, S. R. *J. Org. Chem.* **1999**, *64*, 2505.
(268) Kulkarni, S. A.; Gadre, S. R. *J. Mol. Struct. (THEOCHEM)* **1996**, *361*, 83.
(269) Gadre, S. R.; Pundlik, S. S. *J. Am. Chem. Soc.* **1995**, *117*, 9559.
(270) Gadre, S. R.; Suresh, C. H. *J. Org. Chem.* **1997**, *62*, 2625.
(271) Suresh, C. H.; Gadre, S. R. *J. Am. Chem. Soc.* **1998**, *120*, 7049.
(272) Clar, E. *Polycyclic Hydrocarbons*; Academic Press: London, New York, 1964.
(273) Randic, M. *Chem. Rev.* **2003**, *103*, 3449.
(274) Li, S. H.; Jiang, Y. S. *J. Am. Chem. Soc.* **1995**, *117*, 8401.
(275) Zhou, Z. X.; Parr, R. G. *J. Am. Chem. Soc.* **1989**, *111*, 7371.
(276) Phukan, A. K.; Kalagi, R. P.; Gadre, S. R.; Jemmis, E. D. *Inorg. Chem.* **2004**, *43*, 5824.
(277) Claxton, T. A.; Shirsat, R. N.; Gadre, S. R. *J. Chem. Soc., Chem. Commun.* **1994**, 731.
(278) Peralta-Inga, Z.; Murray, J. S.; Grice, M. E.; Boyd, S.; O'Connor, C. J.; Politzer, P. *J. Mol. Struct. (THEOCHEM)* **2001**, *549*, 147.
(279) Lopez, P.; Mendez, F. *Org. Lett.* **2004**, *6*, 1781.
(280) De Proft, F.; Geerlings, P. *Chem. Rev.* **2001**, *101*, 1451.
(281) Mineva, T.; Heine, T. *J. Phys. Chem. A* **2004**, *108*, 11086.
(282) Pople, J. A. *J. Chem. Phys.* **1956**, *24*, 1111.
(283) Wannere, C. S.; Schleyer, P. v. R. *Org. Lett.* **2003**, *5*, 605.
(284) Viglione, R. G.; Zanasi, R.; Lazzeretti, P. *Org. Lett.* **2004**, *6*, 2265.
(285) Pelloni, S.; Ligabue, A.; Lazzeretti, P. *Org. Lett.* **2004**, *6*, 4451.
(286) Johnson, C. E.; Bovey, F. A. *J. Chem. Phys.* **1958**, *29*, 1012.
(287) Lazzeretti, P. *Prog. Nucl. Magn. Reson. Spectrosc.* **2000**, *36*, 1.
(288) Fowler, J. E.; Jenneskens, L. W. Manuscript in preparation.
(289) Rajagopal, A. K. *J. Phys. C* **1978**, *11*, L943.
(290) Rajagopal, A. K.; Callaway, J. *Phys. Rev. B* **1973**, *7*, 1912.
(291) Gomes, J. *J. Mol. Struct. (THEOCHEM)* **1983**, *10*, 111.
(292) Gomes, J. *Mol. Phys.* **1982**, *47*, 1227.
(293) Gomes, J. *Phys. Rev. A* **1983**, *28*, 559.
(294) Gomes, J. *J. Chem. Phys.* **1983**, *78*, 4585.
(295) Keith, T. A.; Bader, R. F. W. *Chem. Phys. Lett.* **1993**, *210*, 223.
(296) Lipscomb, W. N. *Adv. Magn. Reson.* **1966**, *2*, 137.
(297) Keith, T. A.; Bader, R. F. W. *Chem. Phys. Lett.* **1992**, *194*, 1.
(298) Lazzeretti, P.; Malagoli, M.; Zanasi, R. *J. Mol. Struct. (THEOCHEM)* **1994**, *119*, 299.
(299) Keith, T. A. *Chem. Phys.* **1996**, *213*, 123.
(300) Ditchfield, R. *Mol. Phys.* **1974**, *27*, 789.
(301) Juselius, J.; Sundholm, D.; Gauss, J. *J. Chem. Phys.* **2004**, *121*, 3952.
(302) Gillespie, R. J.; Bayles, D.; Platts, J.; Heard, G. L.; Bader, R. F. W. *J. Phys. Chem. A* **1998**, *102*, 3407.
(303) Karafiloglou, P. *J. Phys. Chem. A* **2001**, *105*, 4524.
(304) Karafiloglou, P.; Panos, C. *Chem. Phys. Lett.* **2004**, *389*, 400.

CR030086P